HHS Public Access

Author manuscript

J Autoimmun. Author manuscript; available in PMC 2016 September 01.

Published in final edited form as:

J Autoimmun. 2015 September ; 63: 31–46. doi:10.1016/j.jaut.2015.06.011.

Distinct and synergistic roles of FcγRIIB deficiency and 129 strain-derived SLAM family proteins in the development of spontaneous germinal centers and autoimmunity

Chetna Soni[a], **Phillip P. Domeier**[a], **Eric B. Wong**[a,1], **Shwetank**[a], **Tahsin N. Khan**[a,2], **Melinda J. Elias**[a], **Stephanie L. Schell**[a], **Aron E. Lukacher**[a], **Timothy K. Cooper**[b], and **Ziaur S.M. Rahman**[a,*]

[a]Microbiology and Immunology, Pennsylvania State University College of Medicine

[b]Departments of Comparative Medicine and Pathology, Pennsylvania State University College of Medicine

Abstract

The inhibitory IgG Fc receptor (FcγRIIB) deficiency and 129 strain-derived signaling lymphocyte activation molecules (129-SLAMs) are proposed to contribute to the lupus phenotype in FcγRIIB-deficient mice generated using 129 ES cells and backcrossed to C57BL/6 mice (B6.129.RIIBKO). In this study, we examine the individual contributions and the cellular mechanisms by which FcγRIIB deficiency and 129-derived SLAM family genes promote dysregulated spontaneous germinal center (Spt-GC) B cell and follicular helper T cell (Tfh) responses in B6.129.RIIBKO mice. We find that B6 mice congenic for the 129-derived SLAM locus (B6.129-SLAM) and B6 mice deficient in FcγRIIB (B6. RIIBKO) have increased Spt-GC B cell responses compared to B6 controls but significantly lower than B6.129.RIIBKO mice. These data indicate that both FcγRIIB deficiency and 129-SLAMs contribute to elevated Spt-GC B cell responses in B6.129.RIIBKO mice. However, only 129-SLAMs contribute significantly to augmented Tfh responses in B6.129.RIIBKO mice, and do so by a combination of T cell-dependent effects and enhanced B cell and DC-dependent antigen presentation to T cells. Elevated Spt-GC B cell responses in mice with FcγRIIB deficiency and polymorphic 129-SLAMs were associated with elevated metabolic activity, improved GC B cell survival and increased differentiation of naïve B cells into GC B cell phenotype. Our data suggest that the interplay between 129-SLAM expression on B cells, T cells and DCs is central to the alteration of the GC tolerance checkpoint, and that deficiency of FcγRIIB on B cells is necessary to augment Spt-GC responses, pathogenic autoantibodies, and lupus disease.

[*]Address correspondence and reprint requests to Dr. Ziaur Rahman, Department of Microbiology and Immunology, H107, Pennsylvania State University College of Medicine, 500 University Drive, Hershey, PA 17033-0850. zrahman@hmc.psu.edu, Ph: (717) 531-0003 × 287896; Fax: (717) 531-6522.

[1]Current address: Department of Blood Cell development & Function, Fox Chase Cancer Center, Philadelphia.

[2]Current address: Department of Molecular Microbiology & Immunology, Oregon Health & Science University

Disclosures

The authors have no financial conflicts of interest.

Keywords

Autoimmunity; Systemic lupus erythematosus; Germinal Centers; Inhibitory IgG receptor FcγIIB; Signaling lymphocyte activation molecules; B cells

1. Introduction

Production of autoantibodies (autoAbs) is a serological hallmark of systemic lupus erythematosus (SLE), a multigenic disorder with genetic predisposition contributing to disease susceptibility [1, 2]. Several mouse models that develop spontaneous (Spt) human SLE-like autoimmunity have been used to delineate the genetic factors involved in the pathogenesis of the disease [2]. Genetic linkage studies in several lupus mouse models (NZB, NZW, NZM2410, BXSB and MRL/*lpr*) have identified at least 31 loci on different chromosomes that contribute to the disease phenotype [3]. The most well studied are the overlapping genetic loci *Sle1* and *Nba-2*, derived from New Zealand White (NZW) and Black (NZB) mice, respectively; *Sle1* and *Nba-2* loci are located on the telomeric region of chromosome 1 [3–7]. B6 mice carrying a similar chromosome 1 region (named *Sle16*) derived from 129/Sv mice also develop lupus-like autoimmunity [8]. This region is syntenic to the human chromosome 1 region 1q22–25, which is also associated with human SLE [9, 10]. Extensive studies on lupus susceptible and non-susceptible mouse strains have identified several polymorphic variations between the two groups in the *Fcγ R* interval and SLAM family genes, located in the *Sle1*/*Nba2*/*Sle16* region [8, 11–13].

Within the *Fcγ R* locus, *Fcgr2b* encodes the low affinity inhibitory receptor for IgG, FcγRIIB, which signals through an immunoreceptor tyrosine based inhibitory motif (ITIM) [14]. FcγRIIB is the only Fc receptor expressed on B cells, functioning to negatively regulate BCR-mediated activation signals [15]. In DCs and other myeloid cells, FcγRIIB opposes the activation signals transduced by the immunoreceptor tyrosine based activation motif (ITAM)-bearing Fc receptors, FcγRI and FcγRIII [16]. FcγRIIB-deficient mice generated using 129/Sv-derived ES cells and backcrossed to C57BL/6 (B6) mice (designated B6.129.RIIBKO) have served as a model for human lupus, exhibiting the accumulation of autoAbs and progression to fatal glomerulonephritis [17, 18].

The close proximity of the FcγRIIB and SLAM family genes located in the *Sle1*/*Nba2*/*Sle16* locus and their involvement in autoimmune susceptibility underlie studies to define the contribution of the FcγRIIB and SLAM family genes to autoimmunity [19–22]. Analysis of B6.129.RIIBKO mice and FcγRIIB-deficient mice generated using B6 ES cells (named B6.RIIBKO) show that the SLAM family genes derived from 129 mice (designated 129-SLAMs) are the major autoimmune susceptibility conferring genes in the *Sle1/Nba2/Sle16* interval, whereas FcγRIIB acts as a modifier of autoimmune susceptibility in B6.129.RIIBKO mice [23]. Verbeek and coworkers (23) found that FcγRIIB deficiency did not contribute to spontaneous autoimmunity on a B6 background. By generating FcγRIIB germline and conditional knockout mice from B6 ES cells, Li et al. recently showed that FcγRIIB is required for maintaining tolerance [24]. However, the cellular mechanisms

regulated by 129-SLAMs and FcγRIIB deficiency, which contribute to lupus pathogenesis in B6.129.RIIBKO mice remain to be defined.

Spontaneously developed germinal centers (Spt-GCs) play a significant role in generating somatically hypermutated and class-switched pathogenic autoAbs, which cause lupus autoimmunity [25–30]. Somatically mutated and pathogenic autoAbs in B6.129.RIIBKO mice have recently been shown to develop through the GC pathway [19], indicating dysregulation at the level of the GC checkpoint. However, the mechanisms by which FcγRIIB deficiency and/or 129-SLAMs contribute to the perturbation of the Spt-GC responses in B6.129.RIIBKO mice are not clear. To determine the cellular functions of various immune cells that may contribute to Spt-GC formation, we compared B6, B6.RIIBKO (FcγRIIB deficient mice generated using B6 ES cells), B6.129-SLAM (B6 mice congenic for the 129-derived SLAM locus) and B6.129.RIIBKO mice (FcγRIIB deficiency on a B6/129 mixed background).

In this study, we provide evidence that both 129-SLAMs and FcγRIIB deficiency independently contribute to the heightened Spt-GC B cell responses in B6.129.RIIBKO mice. 129-SLAMs were found to play a central role in regulating GC Tfh (follicular helper-T cell) responses, which were mostly unaffected by FcγRIIB deficiency. B cells and DCs expressing129-SLAMs had increased antigen presentation capability, and augmented T cell proliferation and functionality. B cells from both B6.129-SLAM and B6.RIIBKO mice showed increased differentiation into GC B cells and improved survival in the GC microenvironment, which was associated with higher energy metabolism than B6 B cells. Our data suggest that the expression of 129-SLAMs on B cells, T cells and DCs was cumulatively important for the observed increase in the Spt-GC and Tfh responses in B6.129-SLAM and B6.129.RIIBKO mice. However, the expression of 129-SLAMs on B cells was particularly important for the selection of autoimmune B cells within GCs. Altogether, this study demonstrates the co-operative yet mutually exclusive roles of FcγRIIB deficiency and 129-SLAMs in altering the GC tolerance checkpoint, leading to the production of autoAbs and lupus pathology.

2. Materials and Methods

2.1 Mice

Breeding pairs for C57BL/6J (B6, stock number 000664), B6.μMT (B6.129S2-*Ighm*^{tm1Cgn}/J, stock number 002288), and OT-II transgenic (B6.Cg-Tg (TcraTcrb)425Cbn/J, stock number 004194) mice were originally purchased from the Jackson Laboratory (Bar Harbor, Maine) and bred in-house. FcγRIIBKO mice (Fcgr2b<tm1.2Rav) were generated on a pure B6 background (B6.RIIBKO) as described [31, 32]. The Ig V_H knock-in mouse line, HKIR (*Igh*^{tm1Tim}), was described previously [33, 34]. B6.129.RIIBKO (B6.129S4-*Fcgr2b*^{tm1TtK} N12, model 580) mice were purchased from the Taconic Farms (Hudson, NY). B6.129-SLAM congenic mice were generated through the transfer of the SLAM locus from 129 to C57BL/6 mice by the marker-assisted speed congenics approach as described [8]. All animals were housed in the barrier mouse facility at Penn State Hershey Medical Center. All experimental procedures were performed in accordance with the guidelines and approved by

the Pennsylvania State University College of Medicine Institutional Animal Care and Use Committee.

2.2 Genetic background analysis

Genetic background analysis of B6.129-SLAM and B6.129.RIIBKO mice was performed using tail DNA samples, on a 1449 SNP Illumina Bead Chip, and analyzed on SNAP-Map software at DartMouse speed congenic core facility, the Geisel School of Medicine, Dartmouth College.

2.3 Flow cytometry reagents

The following antibodies were utilized for flow cytometric analysis of mouse splenocytes: Pacific Blue-anti-B220 (RA3-6B2); Alexa Fluor-700-anti-CD4 (RM4-5); PE-anti-PD-1 (29F.1A12); BV605-anti-CD69 (H1.2F3); Allophycocyanin-anti-TCR-Vα2 (B20.1); Allophycocyanin-Cy7-anti-CD25 (PC61); PeCy7-anti-CD95 (FAS, Jo2); PeCy7-anti-MHC-II (M5/114.15.2); APC-anti-2B4 (m2B4(B6)458.1); APC-anti-CD48 (HM48-1); PerCP-Cy5.5-anti-CD150 (TC15-12F12.2); Biotin-anti-Ly9 (Ly9ab3); Biotin-anti-CD84 (mCD84.7); Pacific Blue-anti-Ly108 (330-AJ) and PE-Cy5-streptavidin (SA) were purchased from BioLegend, San Diego, CA. Biotin-anti-CXCR5 (2G8); FITC-GL7 and FITC-anti-CD11c (HL3) were from BD Pharmingen, San Diego, CA. FITC-peanut-agglutinin (PNA) from Vector Labs, Burlingame, CA. CD16/32 (clone 2.4G2) was from eBiosciences, San Diego, CA. SA-PE conjugate was purchased from Sigma Aldrich, St. Louis, MO. Anti-idiotypic mAb E4, recognizing DNA/Ars dual reactive HKIR B cells [35] and mAb K9.361 (kind gift from Dr. U Hammerling, Sloan-Kettering Memorial Hospital, New York, NY), recognizing FcγRIIB from the B6 background were purified from the respective hybridoma and biotinylated in-house. Stained cells were analyzed using the BD LSR II flow cytometer (BD Biosciences, Franklin lakes, NJ). Data were analyzed using FlowJo software (Tree Star, San Carlos, CA). Dead cells were excluded from analysis by flow cytometry using 4′, 6-diamidino-2-phenylindole exclusion (DAPI) (Sigma-Aldrich, St. Louis, MO). The SR-FLICA *in vitro* caspase detection kit (Poly-caspase SR-VAD-FMK) was purchased from AbD Serotec (Kidlington, U.K.).

2.4 Immunofluorescence and ANA staining

Mouse spleens and kidneys were embedded in OCT compound and snap frozen over liquid nitrogen. 5μm thin sections were cut on a cryostat, mounted on colorfrost plus microscope slides (Fisher Scientific, PA) and fixed in cold acetone for 20 min. The following antibodies and reagents were utilized for immunofluorescence staining of mouse spleen sections for germinal centers: PE-anti-CD4 (GK1.5); FITC-GL7 (RA3-6B2); APC-anti-IgD from BD Biosciences, Franklin lakes, NJ. Kidney sections were stained for C3 using FITC–anti-C3 from Immunology Consultants Laboratory (Portland, OR) or Biotin-anti-IgG (Jackson Immunoresearch). Anti-nuclear Ab (ANA) reactivity was detected by indirect immunofluorescence staining of HEp-2 cell slides (Antibodies Inc., Davis, CA) using sera from indicated mice at a 1:50 dilution, and probed with FITC-rat anti-mouse Kappa (H139-52.1, from Southern Biotechnologies associates, Inc., Birmingham, AL). The images of stained spleen sections were captured using the Leica DM4000 fluorescence microscope

and analyzed using a Leica application suite-advanced fluorescence software (LAS-AF), (Leica Microsystems, Buffalo Grove, IL). For the measurement of GC area, a total of at least 10 randomly selected germinal centers ($GL\text{-}7^+$) per spleen section from at least 5 mice per indicated strain were measured for total area (μm^2) using the LAS-AF quantitation tool. The color intensity of the pseudo-colored images was slightly enhanced using Adobe Photoshop CS4 (Adobe Systems, San Jose, CA). This manipulation was necessary for better visualization, and was carried out consistently between control and test sections while maintaining the integrity of the data.

2.5 RNA-preparation and Real time RT-PCR

Total RNA was isolated from sorted GC Tfh cells from indicated mice or from 40LBNB cultures, using TRIzol reagent (Ambion, Grand Island, NY) following manufacturer's instructions. RNA was reverse transcribed using the high capacity reverse transcription kit (Applied Biosystems, Grand Island, NY). mRNA expression was quantified using the Power SYBR Green PCR master mix kit (Applied Biosystems, Grand Island, NY) on the Applied Biosystems StepOne Plus real time PCR system. Primers were designed using Primer3 software and synthesized by IDT technologies (Coralville, Iowa). Amplification conditions for all primer sets were; one cycle of 95 °C for 10 min, followed by 40 cycles of 95 °C for 15 sec and 60 °C for 1 min. 18srRNA was used as the reference gene for sample normalization. PCR primer details are as follows: PD-1 Forward: 5'-GAG CTC GTG GTA ACA GAG AGA A-3', PD-1 Reverse: 5'- ACA GGG ATA CCC ACT AGG GC-3'; ICOS-Forward: 5'-CGG ATC CAG TGT GCA TGA CC-3', ICOS-Reverse: 5'-AGC TTA TGA GGT CAC ACC TGC-3', 18S rRNA-Forward: 5'-CAC TTT TGG GGC CTT CGT GT-3', 18S rRNA Reverse: 5'-AGG CCC AGA GAC TCA TTT CTT-3', AICDA Forward: 5'-CCT TCG CAA CAA GTC TGG CT-3', AICDA Reverse: 5'-GAA CCA GGT GAC GCG GTA A-3', IL-10 primer 1: 5'-ATG GCC TTG TAG ACA CCT TG-3', IL-10 primer 2: 5'- GTC CTC GAT TTCC TCC CCT GTG-3', IL-4 primer 1: 5'-TCT TTA GGC TTT CCA GGA AGT C-3', IL-4 primer 2: 5'-GAG CTG CAG AGA CTC TTT CG-3', IL-21 primer 1: AGG AGC CAT TTT AGT CTT TCT AGG-3' and IL-21 primer 2: 5' GGA GGA AAG AAA CAG AAG CAC A-3'.

2.6 Immunizations

Eight-10 wk old B6, B6.RIIBKO or B6.129-SLAM mice were immunized (i.p.) with 200μg/mouse ovalbumin (OVA) in alum. Splenocytes were analyzed 12 days after immunization by flow cytometry. Sera samples were analyzed for antibody titers.

2.7 In vitro antigen presentation assay

B cells as APCs—B cells were purified from splenocytes of B6, B6.RIIBKO or B6.129-SLAM mice by negative selection using anti-CD43 (Ly-48) microbeads (Miltenyi Biotec). Purified B cells were stimulated with 20 μg/ml anti-CD40 (clone FGK4.5, UCSF monoclonal Ab core) and 1μg/ml *E.coli* LPS (Sigma Aldrich, St. Louis, MO) for 72h. Thereafter, cells were washed and pulsed with 10 μg/ml OVA-peptide (Inviogen, San Diego, CA) for 6 h. OT-II T cells were purified by negative selection using Pan T cell isolation kit

II (Miltenyi Biotec), labeled with 3μM CFSE, and co-cultured with OVA-peptide loaded B cells for 72–96 h. OT-II T cell activation and proliferation was assessed by flow cytometry.

DCs as APCs—Bone marrow cells harvested from B6, B6.RIIBKO or B6.129-SLAM mice were cultured in 10% DMEM with 10 ng/ml recombinant murine GM-CSF and 10 ng/ml FLT3-L (PeproTech, Rocky Hill, NJ) for two days. The adherent cells were further cultured for 6 days in 10% DMEM supplemented with GM-CSF and FLT3-L, were subsequently trypsinized and analyzed for the F4/80^{lo}, MHC-II^{hi} and CD11c^{hi} DC phenotype by flow cytometry. Subsequently, cells were stimulated with 1 μg/ml *E.coli* LPS (Sigma Aldrich, St. Louis, MO) for 24 h, followed by loading with 10 μg/ml OVA-peptide (323–339) for 6–8 h. OT-II T cells were purified by negative selection using the Pan T cell isolation kit II (Miltenyi Biotec), labeled with 3μM CFSE, and co-cultured with OVA-pulsed DCs for 72–96 h. OT-II T cell activation and proliferation was assessed by flow cytometry and the cell-free culture supernatant was collected for cytokine analysis.

2.8 Cytokine quantification

The culture supernatants from DC-APC- OT-II T cell co-cultures were harvested at indicated time points and used for the quantification of secreted cytokines. Levels of inflammatory cytokines and chemokines were determined by flow cytometry using the BD Cytometric Bead Array (CBA) mouse inflammatory cytokine kit (BD Biosciences, San Jose, CA), as per manufacturer's instructions. The cytokine concentrations were quantified by standard curves plotted employing a five-parameter logistic curve-fitting model, using BD FCAP Array software (Soft Flow Hungary Ltd. for BD Biosciences). Samples with cytokine concentration below the detection limit for the assay were arbitrarily assigned a value of 1 pg/ml.

2.9 In vitro B cell- T cell conjugation assay

Naïve B cells from each indicated group of mice were purified with mouse anti-CD43 (Ly-48) microbeads, stained with 3 μM Cell Trace Violet (Invitrogen, Green Island, NY) and activated with 25 μg/ml soluble anti-IgM (Jackson Immunoresearch) and 1 μg/ml LPS (E.coli LPS, Sigma Aldrich) for 24h h at 37°C in a CO_2 incubator. Simultaneously, naïve T cells from OT-II transgenic mice were purified with a pan-T isolation kit (Miltenyi Biotech), stained with 3 μM CFSE, and activated with 10 μg/ml anti-CD3 (clone 145-2C11, UCSF monoclonal Ab core) and 2 μg/ml anti-CD28 (clone PV-1, UCSF monoclonal Ab core) for 24h. For the last 6 h of stimulation, 10 μg/ml OVA peptide (323–339) (InvivoGen, San Diego, CA) was added to the B cells. Thereafter, B and T cells were washed. 1×10^6 B cells and 1×10^6 T cells were mixed together in a total volume of 100 μl of FACS buffer and briefly centrifuged at 4 °C for 1 min at 1500 rpm. B:T mixtures were then immediately fixed (time-0 min) or incubated in a 37 °C water bath for the indicated time points (2, 5, 15, 30 and 60 min). Interacting B and T cells were co-cross-linked by the addition of 100 μl of 4% paraformaldehyde at the end of each time point. Samples were acquired by flow cytometry.

2.10 In vivo B cell proliferation

Eight-ten week-old female B6.μMT recipient mice were immunized with 200 μl of 10% sheep red blood cells (SRBC) in PBS, 2 days prior to cell transfer. Each mouse received

(i.v.) 5×10^6 CFSE-labeled B cells from splenocytes of female B6, B6.RIIBKO or B6.129-SLAM mice. B cells were purified by negative selection using anti-CD43 (Ly-48) microbeads (Miltenyi Biotec). Splenocytes from recipient mice were analyzed for the proliferation of transferred B cells by CFSE dilution on day 4 after transfer.

2.11 In vitro GC B cell differentiation

In vitro GC B cells were generated using protocols previously described [36]. Briefly, 5×10^5 purified B cells (labeled with 3 μM CFSE) were cultured in a 90 mm tissue culture petriplate (BD Falcon), over an adherent layer of $3–4 \times 10^6$ γ-irradiated (120 Gy) 40LBNB fibroblast cell line, which expresses CD40L and BAFF, for four days. The culture media contained RPMI-1640 medium (Sigma Aldrich), supplemented with 10% FCS, β-ME (5.5×10^{-5} M), HEPES (10 mM), sodium pyruvate (1 mM), 100-units/ml penicillin, and 100-μg/ml streptomycin (GIBCO) and rIL-4 (5 ng/ml; Peprotech, Rocky Hill, NJ). On the 4th day of culture, cells were harvested and analyzed for surface marker expression and/or CFSE dilution by flow cytometry or were processed for RNA preparation.

2.12 Ex vivo apoptosis detection assay

6×10^6 total splenocytes from 3–4 mo old female mice of the indicated strains were stained with SR-FLICA *in vitro* poly-caspase detection reagent for 30 min at 37°C in a water bath, followed by staining with GC B cell markers (B220, PNA, anti-CD95/Fas). Cells were acquired immediately after staining on the BD LSRII cytometer. DAPI positive dead cells and doublets were excluded from the analysis.

2.13 Extracellular flux analysis

Oxygen consumption rate (OCR) and extracellular acidification rate (ECAR) were measured in a XF96 extracellular flux analyzer using a kit following manufacturer's instructions (Seahorse Bioscience, Boston, MA). Briefly, B cells from B6, B6.RIIBKO, B6.129-SLAM and B6.129.RIIBKO mice were purified by negative selection using CD43 microbeads by MACS purification (Miltenyi Biotech). Purified B cells were either used in a naïve state or stimulated with 25 μg/ml anti-IgM and 20 μg/ml anti-CD40 for 18h in RPMI1640 with 10% FCS. 6×10^5 naïve or stimulated B cells (as indicated) were plated in XF seahorse media with 25 mM glucose onto a Cell-TAK (BD Biosciences) coated XF96 plate. Oligomycin (1 μM), carbonyl cyanide 4-(trifluoromethoxy) phenylhydrazone (FCCP, 2 μM), rotenone and antimycin (1 μM each), were added sequentially and measurements of extracellular flux were recorded. Glycolysis was calculated from ECAR values at the basal respiration phase. Glycolytic capacity was calculated from ECAR values after the inhibition of ATP synthase by adding oligomycin, when cells resort to using their maximum glycolytic capacity to meet their energy demands. OCR and ECAR data were analyzed using the XF wave software and plotted using GraphPad prism v6.0.

2.14 Adoptive transfer

HKIR B cell transfer—B6 or B6.129-SLAM recipient female mice were immunized (i.p.) with 100 μg *p*-azophenyl arsonate- keyhole limpet hemocynanin (Ars-KLH)/ mouse (in imject alum, Thermo Scientific, Waltham, MA). Seven days after immunization 2×10^6

MACS-purified splenic B cells from B6.HKIR female donor mice were injected intravenously followed by injection of 50 μg Ars-KLH in PBS (i.p.). Spleens from the recipient mice were harvested 5 days later and evaluated by flow cytometric analysis.

2.15 Serology: Autoantibody titers

Serum autoantibody titers were measured using standard ELISA protocols. ELISA plates were coated with dsDNA (Invitrogen, Green Island, NY), histone (Sigma Aldrich, St. Louis, MO), and nucleosome. IgG subtype-specific autoantibody titers were detected by biotinylated-anti-IgG2b, and AP-anti-IgG2c Abs (Southern Biotech, Birmingham, AL). Biotinylated antibodies were detected by streptavidin (SA) - alkaline phosphatase (Vector Laboratories, Burlingame, CA). The plates were developed with the PNPP (*p*-Nitrophenyl Phosphate, Disodium Salt) (Thermo Fisher Scientific, Rockford, IL) substrate for alkaline phosphatase and read at λ405nm. Serum antibody titers were quantitated as described [37].

2.16 Histopathology

Kidneys were fixed in 10% neutral buffered formalin and embedded in paraffin. Kidney sections of 3μm thickness were cut and stained with periodic acid–Schiff (PAS) reagent according to standard protocols. All images were obtained with an Olympus BX51 microscope and DP71 digital camera using cellSens Standard 1.12 imaging software (Olympus America, Center Valley, PA). A pathologist blinded to the genotype of the mice examined all kidney sections. One kidney section per mouse was evaluated: each individual glomerulus was examined at 400x magnification and scored from 0 (normal) to 4 (severe) based on glomerular size and lobulation, presence of karyorrhectic nuclear debris, capillary basement membrane thickening, and the degree of mesangial matrix expansion and mesangial cell proliferation.

2.17 Statistical analysis

An unpaired, nonparametric, Mann–Whitney, Student *t* test was used to compare two groups, whereas one-way ANOVA or two-way ANOVA (Fig. 4B), followed by the Tukey multiple-comparison test, was used to compare more than two groups. GraphPad Prism 6 software (La Jolla, CA) was used for all the analyses. Error bars reflect mean ± SD, unless otherwise indicated. NS= not significant, * $p \leq 0.05$, ** $p \leq 0.01$, ***$p \leq 0.001$ and **** $p \leq 0.0001$.

3. Results

3.1 Strain origin of FcγRIIB and SLAM in B6.129-SLAM mice

Genome-wide SNP-analysis showed that 0.6% genome in B6.129-SLAM mice and 0.84% in B6.129.RIIBKO mice were derived from 129/Sv mice (Supplementary Fig. 1A), mostly localized on chromosome 1 between 171.3- 176.1 Mb (roughly 4.8 Mb) in B6.129-SLAM mice and between 169.3- 176.1 Mb (6.8 Mb) in B6.129.RIIBKO mice (Supplementary Fig. 1B). This region includes seven members of the SLAM-family genes clustered between 171.3- 172.2 Mb [8]. The tightly linked *Fcγr2b* gene occupies the genomic region from 170.96–170.97 Mb on chromosome 1. However, this region does not contain any distinguishing SNPs between B6 and 129 strains of mice.

To further determine whether B6.129-SLAM mice carry the B6 or 129 allele of FcγRIIB, we stained B cells in 6 mo old B6 and B6.129-SLAM mice with the mAb clone K9.361, which specifically recognizes the B6 allele (Ly17.2 allotype) of FcγRIIB [38]. FcγRIIB expression on $B220^{+}PNA^{-}CD95^{-}$ non-GC (naïve) B cells was comparable between B6 and B6.129-SLAM mice (Fig. 1A, **upper panel**). FcγRIIB expression on $B220^{+}PNA^{+}CD95^{+}$ GC B cells was upregulated in both B6 and B6.129-SLAM mice (Fig.1A, **upper panels**), indicating that FcγRIIB is of B6 origin [38]. Using anti-CD16/CD32 (FcγRII/III) mAb that recognizes both Ly17.1 and Ly17.2 isoforms, we observed downregulation of FcγRIIB on GC B cells from129/SvJ mice, as previously reported [22, 39]. In contrast, GC B cells from B6.129-SLAM mice upregulated FcγRIIB expression like those in B6 mice (Fig. 1A, **lower panels**). B6.129.RIIBKO mice carry an identical SLAM locus to that in B6.129-SLAM mice (Supplementary Figure 1). Six mo old B6 and B6.129-SLAM mice differ in expression of SLAM family members on non-GC B cells, GC B cells, T cells and DCs ($CD11c^{+}$, $MHC\text{-}II^{hi}$) (Fig.1 B-G). These data demonstrate that B6.129-SLAM congenic mice carry the B6 allele of FcγRIIB and 129 allele of the SLAM locus.

3.2 Combined and distinct contributions of FcγRIIB deficiency and 129-SLAMs for Spt-GC B cell responses and Tfh differentiation

Comparison of Spt-GC responses in B6, B6.RIIBKO, B6.129- SLAM and B6.129.RIIBKO mice showed that the frequency of $B220^{+}PNA^{hi}CD95^{hi}$ Spt-GC B cells in 6–7 mo old female mice was B6.129.RIIBKO >> B6.129-SLAM > B6.RIIBKO > B6 mice (Fig. 2A and C), an order paralleling that of splenic GC size (Fig. 2F and G). The percentage of $CD4^{+}CXCR5^{hi}PD\text{-}1^{hi}$ GC Tfh and $CD4^{+}CXCR5^{int}PD\text{-}1^{int}$ Tfh in B6.129-SLAM mice was also significantly higher than in B6 mice, but lower than in B6.129.RIIBKO mice (Fig. 2B, D and E). However, B6.RIIBKO mice did not show a significant increase in GC Tfh and Tfh cell percentages compared to B6 controls (Fig. 2B, D and E). We observed similar results when total cell numbers of GC B cells, GC Tfh and Tfh were analyzed in the four strains of mice (Table 1). Immunofluorescence analysis also revealed that both B6.129.RIIBKO and B6.129-SLAM mice had increased $CD4^{+}GL7^{+}$ GC Tfh cells evidenced by yellow overlapped staining (overlay, Fig. 2F). Although B6.RIIBKO mice had larger GCs than B6 mice, the number of GC Tfh cells was similar to B6 mice (Fig. 2G and F). These data indicate that FcγRIIB deficiency and 129-SLAM proteins together contribute to the development of Spt-GC B cell responses, but 129-SLAM family members are sufficient to regulate differentiation of T cells to the Tfh/GC Tfh phenotype (Fig. 2B, D and E).

We next determined if the increased number and percentage of GC Tfh cells in B6.129-SLAM and B6.129.RIIBKO mice correlated with increased GC Tfh activity and function. Quantitative RT-PCR analysis of sorted GC Tfh cells from 6 mo old B6, B6.RIIBKO, B6.129-SLAM and B6.129.RIIBKO mice revealed that the presence of 129-SLAMs induced more than 5-fold increase in IL-21 transcripts compared to B6 mice (Fig. 2H). Both B6.RIIBKO and B6.129-SLAM GC Tfh cells showed a 5-fold increase in PD-1 expression (Fig. 2H). However, in B6.129.RIIBKO mice, there was a 15-fold increase in mRNA levels of PD-1 and IL-21 and a 3-fold increase in ICOS transcripts compared to B6 GC Tfh (Fig. 2H).

These data suggest that both the deficiency of FcγRIIB and the presence of 129-SLAMs independently cause dysregulation in the Spt-GC B cell response. However, the increase in GC Tfh numbers, and their function is predominantly affected by 129-SLAMs.

3.3 Enhanced antigen presentation by B cells and DCs expressing 129-SLAMs

To determine if differences in Spt-GC responses between B6.RIIBKO and B6.129-SLAM mice were seen after antigenic stimulation, 8–10 wk old B6, B6.RIIBKO and B6.129-SLAM mice were immunized with ovalbumin (OVA). B6.129-SLAM mice had significantly more GC B cells 12 days post-immunization than B6 mice (Fig. 3A). Although not significant, B6.RIIBKO mice trended toward having higher GC B cell responses than B6 mice (Fig. 3A, **left panel**). Similar to the Spt-GC response, the percentage of GC Tfh and Tfh cells was two-fold higher in Ag-induced GCs in B6.129-SLAM mice than B6 and B6.RIIBKO mice (Fig. 3A).

GC B cells may operate as antigen-presenting cells (APCs) within GCs [40]. We found similar MHC-II expression levels on non-GC and GC B cells of OVA-immunized B6, B6.RIIBKO and B6.129-SLAM mice, with significant MHC-II upregulation only on GC B cells from B6.129-SLAM mice (Fig. 3B). Next, B cells sorted from 2 mo old mice were activated, differentiated and pulsed with OVA-peptide (OVA332-339) (designated B-APCs), then co-cultured with CFSE labeled B6.OT-II T cells. A significantly higher percentage of OT-II T cells proliferated following stimulation by B6.RIIBKO or B6.129-SLAM derived B-APCs than by those from B6 mice (Fig. 3C).

Differentiation of T cells into GC Tfh is a multi-step process and involves antigen-specific interaction of T cells with DCs outside of GCs and subsequently with B cells within GCs [41]. Given enhanced Tfh/GC Tfh responses seen in B6.129-SLAM mice (Fig. 2E) we asked whether $OVA_{332–339}$ peptide presentation by DCs (DC-APCs) was altered in the presence of 129-SLAMs or by the absence of FcγRIIB. DC-APCs expressing 129-SLAMs lead to significantly higher proliferation (Fig. 3D and E) and activation of B6.OT-II T cells than B6 and B6.RIIBKO DC-APCs (Fig. 3F). DC-APCs from B6.RIIBKO mice did not induce a higher proliferation rate in B6.OT-II T cells compared to B6 DC-APCs (Fig. 3D and E), although a significant upregulation of surface CD69 and CD25 on OT-II T cells was observed (Fig. 3F). OT-II T cells secreted more TNF-α and IFN-γ in co-cultures with DC-APC from B6.RIIBKO and B6.129-SLAM mice than B6 mice (Fig. 3G). Altogether, both FcγRIIB deficiency and the presence of 129-SLAMs affected B cells and DCs in their ability to present antigen to T cells. B cells and DCs from 129-SLAMs exhibited stronger APC activity.

3.4 Reduced frequency of B and T cell conjugates in B cells deficient in FcγRIIB

Antigen-specific interactions between GC B cells and GC Tfh are important for the survival, proliferation and differentiation of both the cell types [42, 43]. We utilized an *in vitro* flow cytometry-based B and T cell conjugation assay to determine if the B and T cell interactions were modulated by the presence of 129-SLAMs and/or the deficiency of FcγRIIB. Purified B cells from B6, B6.RIIBKO, B6.129-SLAM and B6.129.RIIBKO mice were activated with anti-IgM and LPS and pulsed with OVA peptide to present the peptide and form conjugates

with B6.OT-II T cells specific for $OVA_{323–339}$. We observed no difference in the frequency of B cell: OT-II T cell (B: T) conjugates between B cells derived from B6 and B6.129-SLAM mice (Fig. 4A and B). However, a significantly reduced percentage of B: T conjugates formed when B cells were deficient in FcγRIIB (Fig. 4A and B). B6.129.RIIBKO B cells formed significantly reduced frequency of conjugates than B6 and B6.129-SLAM B cells at all time-points, but significantly more conjugates than B6.RIIBKO at later time points (Fig. 4A and B).

3.5 Both B cell-intrinsic deficiency of FcγRIIB and the expression of 129-SLAMs on B cells promote GC B cell differentiation and survival

Next, we evaluated whether the elevated Spt-GC B cell responses in B6.RIIBKO and B6.129-SLAM mice resulted from an increased proliferation of B cells in the absence of FcγRIIB and/or the presence of 129-SLAMs. CFSE-labeled naïve B cells from 2 mo-old B6, B6.RIIBKO or B6.129-SLAM mice were transferred into μMT mice immunized with sheep red blood cells (SRBC) and the *in vivo* proliferation of these cells in the spleen was assessed. We did not observe any significant differences in the kinetics or percentage of B cell proliferation among the three strains (Fig. 5A and B). Additionally, purified B cells from all the three strains proliferated equally when stimulated with anti-IgM and anti-CD40 *in vitro* for 48–96h (data not shown).

Next, to address if the absence of FcγRIIB and the expression of 129-SLAMs specifically on B cells promoted the differentiation of naïve B cells into GC-like B cells, we used a well-established *in vitro* culture system to differentiate naïve B cells into GC-like B cells [36]. B cells from B6, B6.RIIBKO and B6.129-SLAM mice were cultured on the 40LBNB fibroblast cell line (expressing CD40L and BAFF), and supplemented with IL-4 for 4 days. Consistent with *in vivo* B cell proliferation, naïve B cells from all the three strains proliferated similarly on the 40LBNB cell line (Fig. 5C). However, qPCR analysis revealed a two-fold increase in *Aicda* mRNA transcripts in B cells from B6.RIIBKO and B6.129-SLAM mice (Fig. 5D). Additionally, B cells deficient in FcγRIIB or expressing 129-SLAMs showed a two-fold increase in the surface expression of GL-7 (specific for GC B cells) [44] (Fig. 5E and F). These results indicate that B cell-intrinsic deficiency of FcγRIIB and the expression of 129-SLAMs on B cells promote B cell differentiation into GC B cells.

Increased B cell survival within the GCs can lead to an accumulation of GC B cells [45]. We used an *ex vivo* assay to evaluate the percentage of B cells undergoing apoptosis within the GCs. The percentage of GC B cells undergoing apoptosis was assessed in B6, B6.RIIBKO, B6.129-SLAM and B6.129.RIIBKO mice by measuring the caspase activity in $DAPI^{neg}B220^{+}Fas^{hi}PNA^{hi}$ GC B cells. B6.129.RIIBKO mice had a significantly lower percentage of apoptotic GC B cells than B6 controls (Fig. 5G and H). Although not statistically significant, the percentage of apoptotic GC B cells in B6.RIIBKO and B6.129-SLAM mice appeared to be lower than B6 mice (Fig. 5G and H). These results indicate that the deficiency of inhibitory signals from FcγRIIB and signaling by 129-SLAMs together provide a survival advantage to GC B cells.

3.6 FcγRIIB deficiency enhances energy metabolism in B cells

Growth promoting signals through BCR and growth inhibitory signals through FcγRIIB are shown to modulate B cell glucose energy metabolism [46, 47]. We therefore assessed if the enhancement in GC B cell differentiation and survival observed in B6.RIIBKO, B6.129-SLAM and B6.129.RIIBKO mice was associated with an increased metabolic activity of B cells. We utilized the extracellular flux assay to determine the oxygen consumption rate (OCR; measure of mitochondrial respiration) (Fig. 6A) and extracellular acidification rate (ECAR; measure of glycolysis) (Fig. 6B), in B cells from 3 mo old B6, B6.RIIBKO, B6.129-SLAM and B6.129.RIIBKO female mice. Naïve B cells from B6.129.RIIBKO mice compared with the other three strains showed significantly higher baseline oxygen consumption (Fig. 6C) and ATP production (Fig. 6D). Maximum respiration (Fig. 6E) and spare capacity (Fig. 6F) were also significantly higher in B6.129.RIIBKO mice compared to the other three strains. The average values for the aforementioned parameters were also significantly higher in B cells from B6.RIIBKO mice when compared to B6 controls (Fig. 6A, C, D and E). B6.129-SLAM B cells only showed significant higher ATP production capability when compared to B6 B cells (Fig. 6D). Overall, B6.129-SLAM B cells had moderately higher mitochondrial metabolic function compared to naïve B6 B cells (Fig. 6A). In agreement with a previous study [47], total glycolysis in B cells was enhanced by the deficiency of FcγRIIB (Fig. 6B and G), while B6.129.RIIBKO B cells showed maximum glycolytic capacity among all the four strains (Fig. 6H). Glycolysis and glycolytic capacity of B cells from B6.129-SLAM and B6 mice were not statistically different, but trended to be higher for B6.129-SLAM B cells than B6 B cells (Fig. 6B).

We also measured the mitochondrial respiration (Fig. 6I) and glycolysis (Fig. 6J), in B cells from all the four strains after activation with anti-IgM and anti-CD40 for 18h. Mitochondrial respiratory and glycolytic function was highest in activated B cells from B6.129.RIIBKO mice, followed by B6.RIIBKO and then B6.129-SLAM mice, compared to activated B6 B cells (Fig. 6I). However, activation of B cells from B6.129-SLAM mice resulted in a significant increase in ECAR, more than that in activated B6.RIIBKO B cells, although both were more glycolytically active than activated B6 B cells (Fig. 6J).

These results indicate that FcγRIIB deficiency confers a strong metabolic advantage to B cells. Moreover, 129-SLAMs also cause a modest increase in the glycolytic function of B cells. Thus, FcγRIIB deficiency and 129-SLAMs potentially equip B cells to respond to the high-energy demands within the GC microenvironment, thus presumably resulting in the enhanced survival and differentiation of GC B cells in B6.129.RIIBKO mice.

3.7 B cell-extrinsic expression of 129-SLAMs is not sufficient to drive auto-reactive B cell development in the GCs

Given the role of GC Tfh in spontaneous GC formation and lupus-like autoimmunity [48] we evaluated whether enhanced T cell and/or DC function in the presence of 129-SLAMs could drive autoreactive B cell development in the GCs. We used an adoptive transfer system in which we transferred Ars and DNA-dual-reactive HKIR B cells into syngenic recipients [27, 35, 49, 50]. We previously showed that dual-reactive HKIR B cells can enter GCs upon immunization with Ars-conjugated foreign antigen (i.e., Ars-KLH) but due to

their autoreactivity (DNA-reactivity) these cells are negatively regulated and prevented from expanding in GCs presumably by a GC tolerance checkpoint (40–42). We further demonstrated that B-cell specific expression of NZW-derived *Sle1b* locus harboring SLAM family genes could alter this checkpoint promoting the expansion and selection of Ars-DNA dual-reactive B cells in GCs [27]. In this study, we used the Ars-DNA dual- reactive HKIR B cell system to address if B cell extrinsic expression of 129-SLAMs on T cells and DCs was sufficient to promote HKIR B cell (expressing B6-SLAMs) development within GCs.

We adoptively transferred purified B cells (2×10^6) from B6.HKIR mice into 8–10 wk old sex-matched B6 and B6.129-SLAM mice immunized with Ars-KLH one wk prior to transfer. On day 5 after transfer we determined dual-reactive HKIR B cells in the GCs using the anti-clonotypic mAb E4, specific for HKIR B cells, as described [49]. Consistent with other T-dependent antigenic responses, the total GC response to Ars-KLH was significantly higher in B6.129-SLAM mice when compared to B6 mice (Fig. 7A, **lower panels and** 7B). However, the percentage of Ars-DNA dual reactive HKIR B cells with the GC B cell phenotype (GL-7^+ $E4^+$ B cells) was similar between the two strains (Fig. 7A **lower panels, and** 7B). These data showed that B cell-specific expression of the 129-SLAMs was necessary for autoreactive B cells to expand in the GCs. These results further strengthen our previous findings that the expression of the polymorphic SLAM genes (haplotype-2), in B cells is important for breaking the GC tolerance checkpoint [27].

3.8 FcγRIIB deficiency and 129-SLAMs can independently promote the development of autoAbs and lupus-associated glomerulonephritis

Next, we assessed if the Spt-GC responses in B6.RIIBKO, B6.129-SLAM and B6.129.RIIBKO mice correlated with the development of autoAbs. In accordance with reported literature [18, 19], at 6–7 months of age, B6.129.RIIBKO female mice produced the highest numbers of anti-nuclear Ab (ANA) secreting plasma cells (data not shown) when compared with the other three strains. B6.129.RIIBKO mice also had the highest titers of serum anti-nuclear Abs (ANA) of various IgG subclasses (Fig. 8A–C). Overall ANA titers in B6.RIIBKO and B6.129-SLAM mice were significantly higher than B6 but lower than B6.129.RIIBKO mice (Fig. 8A–C). B6.129-SLAM mice produced higher titers of ANAs than B6.RIIBKO mice (Fig. 8A–C).

To characterize the staining pattern of autoantibodies produced, we analyzed sera from 6–7 mo-old female mice of all four genotypes by indirect immunofluorescence assay on human larynx carcinoma HEp-2 cell line (Fig. 8D). Overall, the fluorescence intensity of positively stained HEp-2 cells was significantly higher in all the three strains compared to B6 controls (Fig. 8E). However, various staining patterns such as nuclear, cytoplasmic and nuclear/cytoplasmic emerged (Fig. 8F). Only faint cytoplasmic staining was observed with a few sera samples from B6 mice. Notably, majority of the B6.RIIBKO mouse sera produced a cytoplasmic staining pattern, whereas more than 50% of the B6.129-SLAM sera stained both the nucleus and cytoplasm of HEp-2 cells. 50% of the B6.129.RIIBKO mice produced nuclear and ≥30% produced nuclear and cytoplasmic staining pattern (Fig. 8F). These data corroborate the previous findings that polymorphic 129-SLAMs contribute significantly to increased anti-nuclear and/or anti-cytoplasmic autoAbs observed in B6.129.RIIBKO mice

[51]. The contribution of FcγRIIB deficiency alone to autoantibody production was previously addressed but conflicting results were reported [20, 23, 24]. We observed a significant effect of FcγRIIB deficiency on a B6 background on AutoAb production. Moreover, an autoantigen array detected high titers of a wide variety of IgG autoAbs against various nuclear and non-nuclear/ cytoplasmic self-antigens in the serum of 6–7 mo old B6.129.RIIBKO mice (Supplementary Fig. 2). Albeit at lower levels than B6.129.RIIBKO mice, many of these autoAbs were also present in B6.RIIBKO mice (Supplementary Fig. 2).

Finally, we addressed if levels of autoAbs correlated with immune-complex-mediated glomerulonephritis (GN) in 7–9 mo-old female B6.RIIBKO, B6.129-SLAM and B6.129.RIIBKO mice. Examination of kidney sections from these mice revealed a significant increase in complement (C3) deposition in B6.129-SLAM, and B6.129.RIIBKO mice when compared to B6 mice (Fig. 9A and B). As previously reported [23], the IgG deposition was higher in both B6.RIIBKO and B6.129.RIIBKO mice than B6.129-SLAM and B6 mice. IgG deposition in the kidneys of B6.129-SLAM mice was significantly higher than B6, but lower than both the FcγRIIB deficient mouse lines (Fig. 9A). All genotypes developed mesangioproliferative glomerulonephritis at this age, ranging from very mild in B6 controls (average score < 1), to mild/moderate in B6.RIIBKO and B6.129-SLAM mice (average score ≥ 1) to severe GN in B6.129.RIIBKO mice (average score > 2) (Fig. 9C and D). Altogether, our data suggest that FcγRIIB deficiency and 129-SLAMs both contribute to a break in the GC tolerance checkpoint leading to the production of class-switched autoAbs and subsequent development of kidney pathology.

4. Discussion

Polymorphisms in the FcγRIIB and SLAM family genes located in the telomeric end of human and mouse chromosome-1 are implicated in autoimmunity [3, 4, 8, 16, 52–54]. The FcγRIIB and SLAM family genes are closely linked, therefore, questions were raised regarding the role of 129-derived SLAM family genes in promoting autoimmune responses in FcγRIIB deficient mice generated using 129 ES cells and backcrossed to B6 mice [17, 18]. The combined and individual contribution of the FcγRIIB and SLAM family genes to autoimmunity were then studied in various spontaneous and induced mouse models of autoimmunity [19–22]. These previous studies suggested that lupus-associated SLAM family genes derived from autoimmune-prone mice contribute to autoimmune responses in these strains [8, 22, 23]. Several previous studies have independently described the modest role of FcγRIIB deficiency and the critical role of 129-SLAMs in enhancing overall autoAb production and related lupus pathology [20, 23, 24, 55]. Here, we defined the effects of FcγRIIB deficiency and the predominant role of 129-SLAM locus in the regulation of Spt-GC B cell and GC Tfh responses. We found that FcγRIIB deficiency and 129-SLAM locus has synergistic, as well as mutually exclusive roles in altering the GC tolerance checkpoint, leading to the production of autoAbs and lupus pathology.

To study the individual and combined effects of FcγRIIB deficiency and 129-SLAMs on GC B cell and Tfh responses, we have compared B6.RIIBKO mice (generated in B6 ES cells) and B6.129-SLAM mice (congenic for 129-derived SLAM locus) with B6.129.RIIBKO mice that are deficient in FcγRIIB and carry the 129-SLAM locus. B6.129-SLAM and

B6.129.RIIBKO mice share an identical SLAM locus, but the 129-derived region in B6.129.RIIBKO mice is ∼2 Mb longer than that in B6.129-SLAM mice. This ∼2 Mb region encompasses *Sh2d1b1, Sh2d1b2, Fcgr2b, Fcgr3 and Fcer1g* immune-related genes. Comparative studies of FcγRIIB- and FcγRIII-deficient mice on a B6.129 background have previously established the greater contribution of FcγRIIB than FcγRIII to the autoimmune phenotype in these mice [23], but cannot exclude the contribution of these genes to the lupus phenotype observed in B6.129.RIIBKO mice. The 129-SLAM genes predominantly mediate the GC responses observed in B6.129-SLAM mice, because the FcγR locus in these mice is of B6 origin (Fig. 1A). This is consistent with our recent report showing that the NZW-derived polymorphic SLAM family genes CD84 and Ly108 in the *Sle1b* sub-locus alter GC B cell tolerance [45]. Other genes downstream of the SLAM locus, including *Ifi202b* and *Ifi204*, have previously been shown not to affect B cell tolerance and autoAb production [56]. Therefore the B6.129-SLAM mouse model is a good model to study the predominant role of 129-SLAM family genes in the dysregulation of GC B cell and Tfh responses and autoimmunity.

Beginning at three mo of age, B6.129-SLAM and B6.129.RIIBKO mice show a significant increase in GC B cell and GC Tfh responses compared to B6 and B6.RIIBKO mice (data not shown). At six mo of age, these differences are pronounced and at this age B6.RIIBKO mice also show a significant increase in the Spt-GC B cell response but not GC Tfh response compared to B6 controls (Fig. 2A–G). This increase in the Spt-GC B cell response is not in line with our previous study where we showed that plasma cell and not the GC B cell number was affected by the FcγRIIB deficiency [35]. This difference in GC B cell response may have resulted from the use of two different model systems. In our previous report, we used an antigen-induced GC model where we transferred arsonate and DNA-dual-reactive HKIR B cells deficient in FcγRIIB and showed an increased number of plasma cells in mice that received HKIR/FcγRIIBKO B cells compared to HKIR B cells (34). In the current study, we determined the effect of FcγRIIB on the Spt-GC responses. Consistent with the antigen-induced GC-HKIR model, we do not observe a significant increase in percentage of GC B cells in B6.RIIBKO mice immunized with T-dependent antigens (Fig. 3A). Li et al. showed increased anti-NP and spontaneous anti-nuclear IgG Ab responses in B6 mice in which Fcγr2b gene is conditionally deleted in GC B cells [24]. They have not, however, examined either induced or spontaneous GC B cell and Tfh responses in these mice. Consistent with our observations, a recent study by Takai and co-workers reported enhanced Spt-GC B cell formation in the presence of 129-SLAM genes alone [57]. However, this study did not examine the effect of 129-SLAMs on Tfh formation and functions. They also have not determined the cellular mechanisms regulated by 129-SLAMs or FcγRIIB to enhance GC responses and autoAb production.

The SLAM family members and their expression and functions in the context of T cells are well documented [12, 53, 54]. In this study, we focused on understanding the role of 129-SLAM proteins expressed on B cells and DCs and their potential contribution to GC B cell and GC Tfh expansion and functional dysregulation. We find significant enhancement in antigen presentation by B cells and DCs expressing 129-SLAMs compared to those expressing B6-SLAMs (Fig. 3B–F). Compared to B6 controls, B cell and DC dependent

antigen presentation were also increased in the absence of FcγRIIB (Fig. 3B–F). Our observation of enhanced T cell activation and pro-inflammatory cytokine production (TNFα and IFNγ) by DCs deficient in FcγRIIB (Fig. 3G) is supported by previous studies showing that FcγRIIB expression on DCs regulates antigen presentation and $CD8^+$ T cell responses [24, 58]. Altered DC function and cytokine production was also previously reported in mice carrying the FcγR and SLAM intervals derived from the *Nba2* locus (22). Taken together with previous reports (22, 37, 55), our data suggests possible mechanisms by which FcγRIIB deficiency and 129-SLAM expression alters the regulation of DC-mediated T cell activation and commitment to Tfh differentiation during Spt-GC development.

Signaling through the SLAM-receptors has been shown to regulate B and T cell interactions [12, 59]. We reasoned that the increased antigen presentation by 129-SLAM-expressing B cells could be due to improved interactions with T cells. While the nature and duration of B and T cell interactions are not clear, we do not find differences in the frequency of B and T cell conjugate formation between B cells expressing 129-SLAMs or B cells expressing B6-SLAMs with B6.OT-II T cells (Fig. 4). Interestingly, we observed a significantly lower frequency of conjugate formation when B cells were deficient in FcγRIIB (Fig. 4), even though antigen presentation and T cell proliferation by B cells deficient in FcγRIIB is enhanced compared to B6 controls (Fig. 3B and C). One possible explanation is that the hyperactivated state of B cells in the absence of FcγRIIB may require only transient interactions with T cells. This lower frequency of conjugate formation may lead to unaltered numbers of GC Tfh cells in B6.RIIBKO mice despite having more GC B cells than B6 mice (Fig. 4 and Fig. 2A, C). However, unlike in B6.RIIBKO mice, the percentage of Tfh and GC Tfh cells was significantly increased in B6.129-SLAM and B6.129.RIIBKO mice, supporting the role of 129-SLAMs in Tfh and GC Tfh expansion and dysregulation (Fig. 2B, D and E). Consistent with this notion we observed a markedly increased mRNA expression of *Pdcd-1*, *Icos*, *Il4* and *Il21* in GC Tfh cells from B6.129.RIIBKO mice (Fig. 2H).

Using an *in vitro* GC B cell differentiation system, we find that B cell intrinsic expression of 129-SLAMs or FcγRIIB deficiency regulates differentiation of naïve B cell into GC-like B cells (Fig. 5 D-F). The survival and selection of GC B cells within the GCs are dependent on BCR signaling and survival signals from GC Tfh [41, 60]. In the absence of survival signals, autoreactive B cells that are likely to arise in GCs due to the random process of somatic hypermutation undergo negative selection via apoptosis. Although not statistically significant, we observe that 129-SLAMs and FcγRIIB deficiency individually contribute to a modest decrease in the percentage of GC B cells undergoing apoptosis. However, we do find a significantly reduced percentage of apoptotic GC B cells in B6.129.RIIBKO mice (Fig. 5G and H). Our data support the possibility that GC Tfh cells expressing 129-SLAMs are functionally more active and produce cytokines like IL-21, which can drive GC B cell differentiation and alter negative selection (Fig. 2H). Additionally, we find that FcγRIIB deficiency and 129-SLAM expression can enhance the energy metabolism in B cells (Fig. 6). Supporting our observations, Rathmell and co-workers recently reported that B cells from autoimmune BAFF Tg mice are metabolically more active, with increased glycolytic efficiency that was necessary for autoAb production [61].

Altogether, lower B cell activation threshold due to FcγRIIB deficiency [14, 15], coupled with better survival cues from 129-SLAM expressing GC Tfh and enhanced energy metabolism, can promote the survival of autoreactive GC B cells leading to their accumulation and production of autoAbs. Consistent with previous reports [18, 19], and the recent report by Kanari et al., [57], we also observe that B6.129.RIIBKO mice develop pathogenic autoAbs and lupus nephritis. In line with the effects of 129-SLAMs and FcγRIIB deficiency on Spt-GC responses, we observe an independent effect of each of them on the accumulation of class-switched autoAbs, further suggesting the generation of autoreactive B cells through the GCs (Fig. 8). Our observations are strengthened by the studies from Takai and group, where they report a modest but significant increase in the accumulation of class-switched ANAs in mice deficient in FcγRIIB or expressing 129-SLAMs [57]. Consistent with their findings [57] we observe a significant contribution of FcγRIIB and not 129-SLAMs in the regulation of IgG deposition in the kidneys (Fig. 9A), supporting the role of FcγRIIB expression on renal mesangial cells in the clearance of IgG from kidneys [62]. Our data also show that B cell-extrinsic expression of 129-SLAMs is not sufficient for driving autoreactive B cell development in the GCs (Fig.7). Thus, 129-SLAM expression on B cells, together with DCs and T cells, may contribute to the loss of GC B cell tolerance in B6.129.RIIBKO mice.

In conclusion, our studies define a prominent B cell-intrinsic role of 129-SLAMs in the dysregulation of the germinal center pathway, by promoting GC B cell differentiation and survival. Our data also indicate that in conjunction with the T cell-specific effects of 129-SLAMs on GC-Tfh functions, 129-SLAMs enhance antigen presentation by B cells, further affecting GC Tfh functions. Additionally, we demonstrate that FcγRIIB deficiency confers higher GC B cell differentiation capacity, increased metabolism and survival advantages to B cells. The independent effects of 129-SLAMs and FcγRIIB deficiency are sufficient to perturb GC B cell selection and generate significantly higher titers of autoAbs. However, the synergistic effects of both 129-SLAMs and FcγRIIB deficiency can lead to the pathogenic accumulation of autoAbs and lupus nephritis.

Supplementary Material

Refer to Web version on PubMed Central for supplementary material.

Acknowledgements

These studies were supported by a grant from the NIH (AI091670) to Z.S.M.R. We thank Drs. Jinchun Zhou and Quan-Zhen Li from UT southwestern microarray core facility for assisting with the autoantigen array. We thank the Penn State Hershey Medical Center flow cytometry core facility and the histopathology staff for their service. We also thank Dr. Sathibabu Chodisetti for valuable discussions and help.

Non standard abbreviations

GC	germinal center
Spt-GC	spontaneous germinal center
PNA	peanut agglutinin

ANA	anti-nuclear antibody
SRBC	sheep red blood cells
Tfh	follicular helper T cells
SLE	systemic lupus erythematosus
CFSE	carboxyfluorescein succinimidyl ester
SLAM	signaling lymphocyte activation molecule

References

1. Wakeland EK, Liu K, Graham RR, Behrens TW. Delineating the genetic basis of systemic lupus erythematosus. Immunity. 2001; 15:397–408. [PubMed: 11567630]
2. Fairhurst AM, Wandstrat AE, Wakeland EK. Systemic lupus erythematosus: multiple immunological phenotypes in a complex genetic disease. Adv Immunol. 2006; 92:1–69. [PubMed: 17145301]
3. Wakeland EK, Wandstrat AE, Liu K, Morel L. Genetic dissection of systemic lupus erythematosus. Current opinion in immunology. 1999; 11:701–707. [PubMed: 10631557]
4. Morel L, Blenman KR, Croker BP, Wakeland EK. The major murine systemic lupus erythematosus susceptibility locus, Sle1, is a cluster of functionally related genes. Proc Natl Acad Sci U S A. 2001; 98:1787–1792. [PubMed: 11172029]
5. Mohan C, Alas E, Morel L, Yang P, Wakeland EK. Genetic dissection of SLE pathogenesis. Sle1 on murine chromosome 1 leads to a selective loss of tolerance to H2A/H2B/DNA subnucleosomes. J Clin Invest. 1998; 101:1362–1372. [PubMed: 9502778]
6. Rozzo SJ, Vyse TJ, Drake CG, Kotzin BL. Effect of genetic background on the contribution of New Zealand black loci to autoimmune lupus nephritis. Proc Natl Acad Sci U S A. 1996; 93:15164–15168. [PubMed: 8986781]
7. Gubbels MR, Jorgensen TN, Metzger TE, Menze K, Steele H, Flannery SA, et al. Effects of MHC and gender on lupus-like autoimmunity in Nba2 congenic mice. Journal of immunology. 2005; 175:6190–6196.
8. Wandstrat AE, Nguyen C, Limaye N, Chan AY, Subramanian S, Tian XH, et al. Association of extensive polymorphisms in the SLAM/CD2 gene cluster with murine lupus. Immunity. 2004; 21:769–780. [PubMed: 15589166]
9. Tsao BP, Cantor RM, Kalunian KC, Chen CJ, Badsha H, Singh R, et al. Evidence for linkage of a candidate chromosome 1 region to human systemic lupus erythematosus. J Clin Invest. 1997; 99:725–731. [PubMed: 9045876]
10. Moser KL, Neas BR, Salmon JE, Yu H, Gray-McGuire C, Asundi N, et al. Genome scan of human systemic lupus erythematosus: evidence for linkage on chromosome 1q in African-American pedigrees. Proc Natl Acad Sci U S A. 1998; 95:14869–14874. [PubMed: 9843982]
11. Smith KG, Clatworthy MR. FcgammaRIIB in autoimmunity and infection: evolutionary and therapeutic implications. Nat Rev Immunol. 2010; 10:328–343. [PubMed: 20414206]
12. Cannons JL, Tangye SG, Schwartzberg PL. SLAM family receptors and SAP adaptors in immunity. Annu Rev Immunol. 2011; 29:665–705. [PubMed: 21219180]
13. Wang A, Batteux F, Wakeland EK. The role of SLAM/CD2 polymorphisms in systemic autoimmunity. Current opinion in immunology. 2010; 22:706–714. [PubMed: 21094032]
14. Bolland S, Ravetch JV. Inhibitory pathways triggered by ITIM-containing receptors. Adv Immunol. 1999; 72:149–177. [PubMed: 10361574]
15. Bolland S, Pearse RN, Kurosaki T, Ravetch JV. SHIP modulates immune receptor responses by regulating membrane association of Btk. Immunity. 1998; 8:509–516. [PubMed: 9586640]
16. Nimmerjahn F, Ravetch JV. Fcgamma receptors as regulators of immune responses. Nat Rev Immunol. 2008; 8:34–47. [PubMed: 18064051]

17. Takai T, Ono M, Hikida M, Ohmori H, Ravetch JV. Augmented humoral and anaphylactic responses in Fc gamma RII-deficient mice. Nature. 1996; 379:346–349. [PubMed: 8552190]
18. Bolland S, Ravetch JV. Spontaneous autoimmune disease in Fc(gamma)RIIB-deficient mice results from strain-specific epistasis. Immunity. 2000; 13:277–285. [PubMed: 10981970]
19. Tiller T, Kofer J, Kreschel C, Busse CE, Riebel S, Wickert S, et al. Development of self-reactive germinal center B cells and plasma cells in autoimmune Fc gammaRIIB-deficient mice. J Exp Med. 2010; 207:2767–2778. [PubMed: 21078890]
20. Sato-Hayashizaki A, Ohtsuji M, Lin Q, Hou R, Ohtsuji N, Nishikawa K, et al. Presumptive role of 129 strain-derived Sle16 locus in rheumatoid arthritis in a new mouse model with Fcgamma receptor type IIb-deficient C57BL/6 genetic background. Arthritis Rheum. 2011; 63:2930–2938. [PubMed: 21953083]
21. Fujii T, Hou R, Sato-Hayashizaki A, Obata M, Ohtsuji M, Ikeda K, et al. Susceptibility loci for the defective foreign protein-induced tolerance in New Zealand Black mice: implication of epistatic effects of Fcgr2b and Slam family genes. Eur J Immunol. 2011; 41:2333–2340. [PubMed: 21604261]
22. Jorgensen TN, Alfaro J, Enriquez HL, Jiang C, Loo WM, Atencio S, et al. Development of murine lupus involves the combined genetic contribution of the SLAM and FcgammaR intervals within the Nba2 autoimmune susceptibility locus. Journal of immunology. 2010; 184:775–786.
23. Boross P, Arandhara VL, Martin-Ramirez J, Santiago-Raber ML, Carlucci F, Flierman R, et al. The inhibiting Fc receptor for IgG, FcgammaRIIB, is a modifier of autoimmune susceptibility. Journal of immunology. 2011; 187:1304–1313.
24. Li F, Smith P, Ravetch JV. Inhibitory Fcgamma receptor is required for the maintenance of tolerance through distinct mechanisms. Journal of immunology. 2014; 192:3021–3028.
25. Shlomchik MJ, Marshak-Rothstein A, Wolfowicz CB, Rothstein TL, Weigert MG. The role of clonal selection and somatic mutation in autoimmunity. Nature. 1987; 328:805–811. [PubMed: 3498121]
26. Meffre E, Wardemann H. B-cell tolerance checkpoints in health and autoimmunity. Curr Opin Immunol. 2008; 20:632–638. [PubMed: 18848883]
27. Wong EB, Khan TN, Mohan C, Rahman ZS. The lupus-prone NZM2410/NZW strain-derived Sle1b sublocus alters the germinal center checkpoint in female mice in a B cell-intrinsic manner. Journal of immunology. 2012; 189:5667–5681.
28. Soni C, Wong EB, Domeier PP, Khan TN, Satoh T, Akira S, et al. B cell-intrinsic TLR7 signaling is essential for the development of spontaneous germinal centers. Journal of immunology. 2014; 193:4400–4414.
29. Jackson SW, Scharping NE, Kolhatkar NS, Khim S, Schwartz MA, Li QZ, et al. Opposing impact of B cell-intrinsic TLR7 and TLR9 signals on autoantibody repertoire and systemic inflammation. Journal of immunology. 192:4525–4532.
30. Brink R. The imperfect control of self-reactive germinal center B cells. Current opinion in immunology. 2014; 28:97–101. [PubMed: 24686094]
31. Li F, Ravetch JV. Inhibitory Fcgamma receptor engagement drives adjuvant and anti-tumor activities of agonistic CD40 antibodies. Science. 2011; 333:1030–1034. [PubMed: 21852502]
32. Smith P, DiLillo DJ, Bournazos S, Li F, Ravetch JV. Mouse model recapitulating human Fcgamma receptor structural and functional diversity. Proc Natl Acad Sci U S A. 2012; 109:6181–6186. [PubMed: 22474370]
33. Heltemes-Harris L, Liu X, Manser T. Progressive surface B cell antigen receptor down-regulation accompanies efficient development of antinuclear antigen B cells to mature, follicular phenotype. Journal of immunology. 2004; 172:823–833.
34. Notidis E, Heltemes L, Manser T. Dominant, hierarchical induction of peripheral tolerance during foreign antigen-driven B cell development. Immunity. 2002; 17:317–327. [PubMed: 12354384]
35. Rahman ZS, Alabyev B, Manser T. FcgammaRIIB regulates autoreactive primary antibody-forming cell, but not germinal center B cell, activity. Journal of immunology. 2007; 178:897–907.
36. Nojima T, Haniuda K, Moutai T, Matsudaira M, Mizokawa S, Shiratori I, et al. In-vitro derived germinal centre B cells differentially generate memory B or plasma cells in vivo. Nature communications. 2011; 2:465.

37. Wong EB, Khan TN, Mohan C, Rahman ZS. The lupus-prone NZM2410/NZW strain-derived Sle1b sublocus alters the germinal center checkpoint in female mice in a B cell-intrinsic manner. J Immunol. 189:5667–5681. [PubMed: 23144494]
38. Rahman ZS, Manser T. Failed up-regulation of the inhibitory IgG Fc receptor Fc gamma RIIB on germinal center B cells in autoimmune-prone mice is not associated with deletion polymorphisms in the promoter region of the Fc gamma RIIB gene. Journal of immunology. 2005; 175:1440–1449.
39. Rahman ZS, Niu H, Perry D, Wakeland E, Manser T, Morel L. Expression of the autoimmune Fcgr2b NZW allele fails to be upregulated in germinal center B cells and is associated with increased IgG production. Genes Immun. 2007; 8:604–612. [PubMed: 17713556]
40. Jackson SW, Kolhatkar NS, Rawlings DJ. B cells take the front seat: dysregulated B cell signals orchestrate loss of tolerance and autoantibody production. Current opinion in immunology. 2015; 33C:70–77. [PubMed: 25679954]
41. Crotty S. T follicular helper cell differentiation, function, and roles in disease. Immunity. 2014; 41:529–542. [PubMed: 25367570]
42. Zotos D, Tarlinton DM. Determining germinal centre B cell fate. Trends in immunology. 2012; 33:281–288. [PubMed: 22595532]
43. Liu D, Xu H, Shih C, Wan Z, Ma X, Ma W, et al. T-B-cell entanglement and ICOSL-driven feed-forward regulation of germinal centre reaction. Nature. 2015; 517:214–218. [PubMed: 25317561]
44. Naito Y, Takematsu H, Koyama S, Miyake S, Yamamoto H, Fujinawa R, et al. Germinal center marker GL7 probes activation-dependent repression of N-glycolylneuraminic acid, a sialic acid species involved in the negative modulation of B-cell activation. Molecular and cellular biology. 2007; 27:3008–3022. [PubMed: 17296732]
45. Wong EB, Soni C, Chan AY, Domeier PP, Shwetank Abraham T, et al. B Cell-Intrinsic CD84 and Ly108 Maintain Germinal Center B Cell Tolerance. Journal of immunology. 2015
46. Doughty CA, Bleiman BF, Wagner DJ, Dufort FJ, Mataraza JM, Roberts MF, et al. Antigen receptor-mediated changes in glucose metabolism in B lymphocytes: role of phosphatidylinositol 3-kinase signaling in the glycolytic control of growth. Blood. 2006; 107:4458–4465. [PubMed: 16449529]
47. Dufort FJ, Bleiman BF, Gumina MR, Blair D, Wagner DJ, Roberts MF, et al. Cutting edge: IL-4-mediated protection of primary B lymphocytes from apoptosis via Stat6-dependent regulation of glycolytic metabolism. Journal of immunology. 2007; 179:4953–4957.
48. Lee SK, Silva DG, Martin JL, Pratama A, Hu X, Chang PP, et al. Interferon-gamma excess leads to pathogenic accumulation of follicular helper T cells and germinal centers. Immunity. 2012; 37:880–892. [PubMed: 23159227]
49. Alabyev B, Rahman ZS, Manser T. Quantitatively reduced participation of anti-nuclear antigen B cells that down-regulate B cell receptor during primary development in the germinal center/memory B cell response to foreign antigen. Journal of immunology. 2007; 178:5623–5634.
50. Vuyyuru R, Mohan C, Manser T, Rahman ZS. The lupus susceptibility locus Sle1 breaches peripheral B cell tolerance at the antibody-forming cell and germinal center checkpoints. Journal of immunology. 2009; 183:5716–5727.
51. Carlucci F, Cortes-Hernandez J, Fossati-Jimack L, Bygrave AE, Walport MJ, Vyse TJ, et al. Genetic dissection of spontaneous autoimmunity driven by 129-derived chromosome 1 Loci when expressed on C57BL/6 mice. Journal of immunology. 2007; 178:2352–2360.
52. Nimmerjahn F, Ravetch JV. Fcgamma receptors: old friends and new family members. Immunity. 2006; 24:19–28. [PubMed: 16413920]
53. Veillette A. SLAM Family Receptors Regulate Immunity with and without SAP-related Adaptors. J Exp Med. 2004; 199:1175–1178. [PubMed: 15123741]
54. Veillette A, Latour S. The SLAM family of immune-cell receptors. Current opinion in immunology. 2003; 15:277–285. [PubMed: 12787752]
55. Bygrave AE, Rose KL, Cortes-Hernandez J, Warren J, Rigby RJ, Cook HT, et al. Spontaneous autoimmunity in 129 and C57BL/6 mice-implications for autoimmunity described in gene-targeted mice. PLoS Biol. 2004; 2:E243. [PubMed: 15314659]

56. Erickson LD, Lin LL, Duan B, Morel L, Noelle RJ. A genetic lesion that arrests plasma cell homing to the bone marrow. Proc Natl Acad Sci U S A. 2003; 100:12905–12910. [PubMed: 14555759]

57. Kanari Y, Sugahara-Tobinai A, Takahashi H, Inui M, Nakamura A, Hirose S, et al. Dichotomy in FcgammaRIIB deficiency and autoimmune-prone SLAM haplotype clarifies the roles of the Fc receptor in development of autoantibodies and glomerulonephritis. BMC immunology. 2014; 15:47. [PubMed: 25339546]

58. Van Montfoort N, t Hoen PA, Mangsbo SM, Camps MG, Boross P, Melief CJ, et al. Fcgamma receptor IIb strongly regulates Fcgamma receptor-facilitated T cell activation by dendritic cells. Journal of immunology. 2012; 189:92–101.

59. Cannons JL, Qi H, Lu KT, Dutta M, Gomez-Rodriguez J, Cheng J, et al. Optimal germinal center responses require a multistage T cell:B cell adhesion process involving integrins, SLAM-associated protein, and CD84. Immunity. 2010; 32:253–265. [PubMed: 20153220]

60. Goenka R, Matthews AH, Zhang B, O'Neill PJ, Scholz JL, Migone TS, et al. Local BLyS production by T follicular cells mediates retention of high affinity B cells during affinity maturation. J Exp Med. 2013; 211:45–56. [PubMed: 24367004]

61. Caro-Maldonado A, Wang R, Nichols AG, Kuraoka M, Milasta S, Sun LD, et al. Metabolic reprogramming is required for antibody production that is suppressed in anergic but exaggerated in chronically BAFF-exposed B cells. Journal of immunology. 2014; 192:3626–3636.

62. Sharp PE, Martin-Ramirez J, Mangsbo SM, Boross P, Pusey CD, Touw IP, et al. FcgammaRIIb on myeloid cells and intrinsic renal cells rather than B cells protects from nephrotoxic nephritis. Journal of immunology. 2013; 190:340–348.

Highlights

- FcγRIIB deficiency and 129-SLAMs promote GC B cell differentiation and survival
- 129-SLAMs and not FcγRIIB deficiency enhances Spt-Tfh formation
- 129-SLAMs on B cells and DCs promote antigen presentation
- FcγRIIB deficient B cells have higher energy metabolism & altered B-T interactions
- Both FcγRIIB deficiency and 129-SLAMs contribute to ANA production

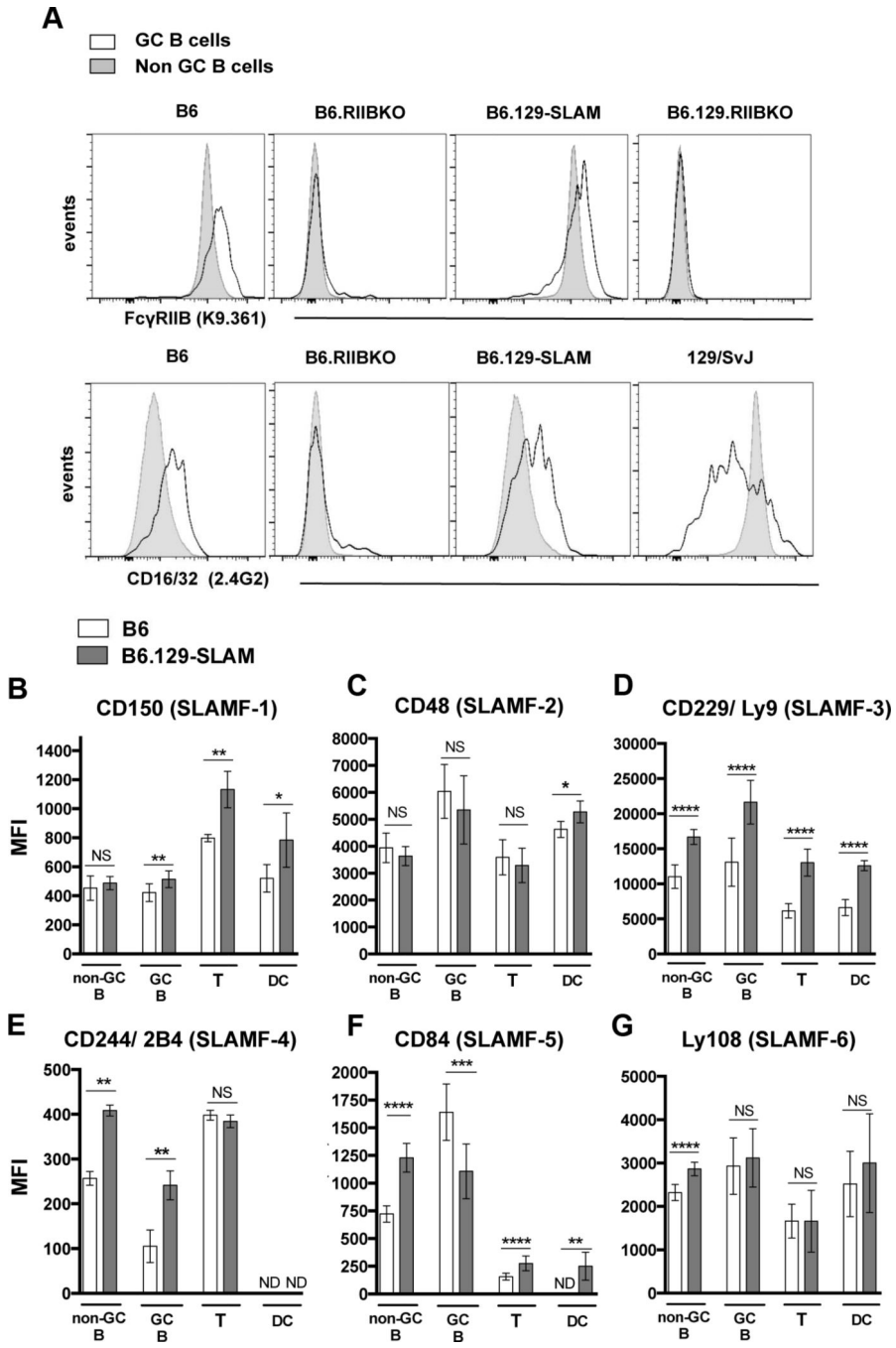

Figure 1. Comparative analysis of FcγRIIB and SLAM cell surface expression in B6 and B6.129-SLAM mice

(A) Histograms show levels of FcγRIIB on $B220^{+}$ splenic non-GC B cells (solid fill) and $B220^{+}PNA^{hi}CD95^{hi}$ GC B cells (no fill) in 6 mo-old female mice of indicated mouse strains. FcγRIIB expression on B cells was detected using the mAb K9.361 specific for the B6 allele of FcγRIIB (upper panels) and by Abs against FcγRII/III (CD16/32, 2.4G2, lower panels). Data are representative of three independent experiments with 4–5 mice per group. **(B–G)** Splenic non-GC B cells, GC B cells, T cells ($CD4^{+}$) and DCs ($CD11c^{hi}MHC\text{-}II^{hi}$)

from 6 mo old female mice were surface stained for CD150 (C); CD48 (D); Ly9 (E); 2B4 (F); CD84 (G) and Ly108 (H) and analyzed by flow cytometry. The mean fluorescence intensity of SLAM molecule expression on each population of cells is shown in bar graphs. At least 6–10 mice were analyzed per data set. Error bars in B-H show mean ± SD. NS= not significant, * $p \leq 0.05$, ** $p \leq 0.01$, ***$p \leq 0.001$ and **** $p \leq 0.0001$ (Mann Whitney t-test).

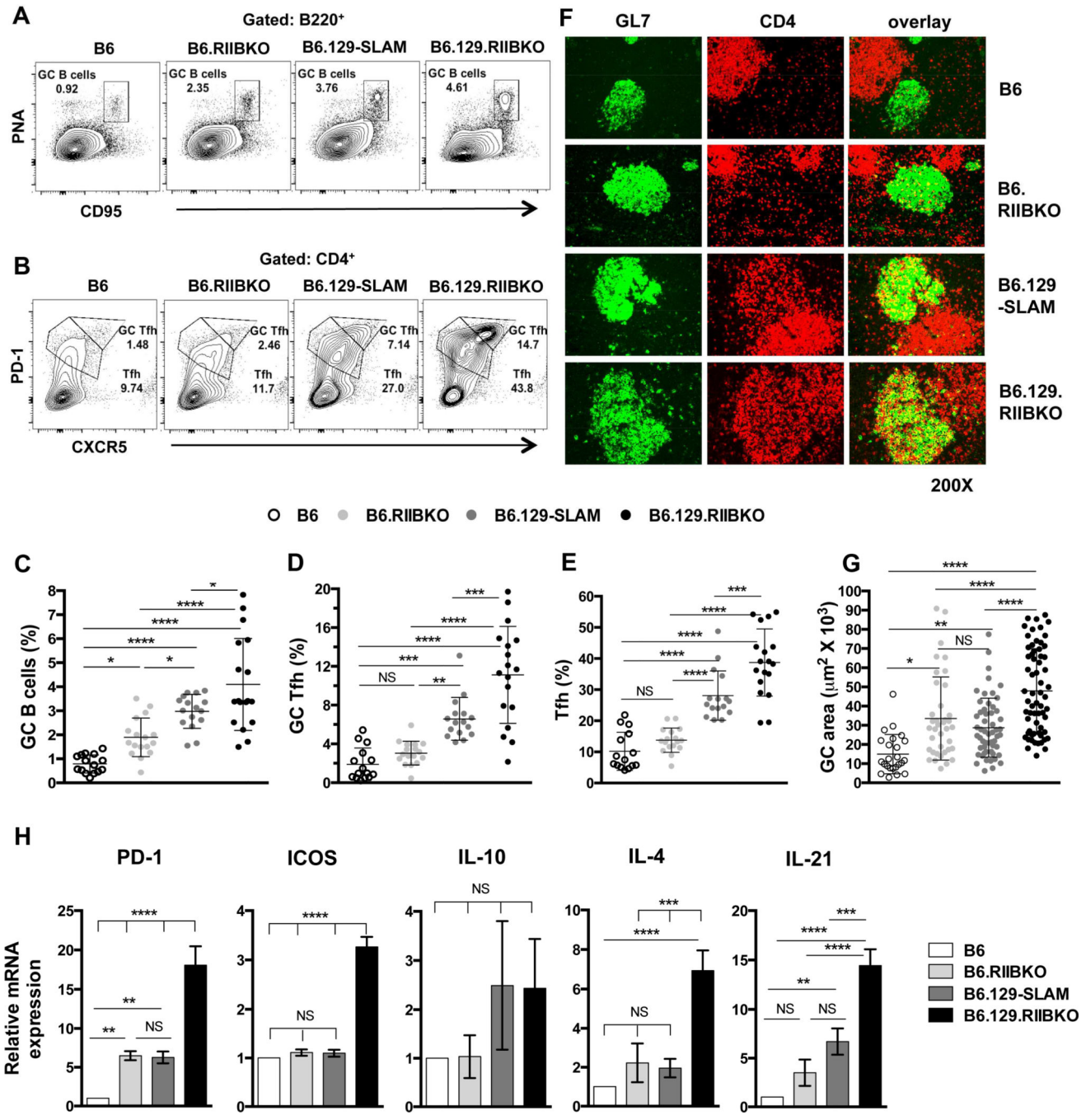

Figure 2. Analysis of GC B cells, Tfh and GC Tfh in B6, B6.RIIBKO, B6.129-SLAM and B6.129.RIIBKO mice

(**A**) Representative contour plots show the gating strategy for $B220^{+}PNA^{hi}$ $CD95^{hi}$ GC B cells (rectangular gate) in 6 mo old female mice of the indicated strains. (**B**) Similar analysis as in (A) showing the gating strategy for Tfh ($CD4^{+}CXCR5^{int}PD\text{-}1^{int}$, lower polygonal gate) and GC Tfh ($CD4^{+}CXCR5^{hi}PD\text{-}1^{hi}$, upper polygonal gate). Scatter plots show the percentage of GC B cells **(C)**, GC Tfh **(D)** and Tfh **(E)** in total splenocytes from 6 mo old female mice of the indicated strains. Each symbol in C, D and E represents an individual

mouse. **(F)** Representative images of spleen sections from 6 mo old mice, stained with fluorescently labeled Abs detecting GC B cells (GL7-green, left panels) and $CD4^+$ T cells (red, middle panels). Right panels show the overlay of GL7 and CD4 staining. Immunofluorescence data are representative of at least 5–6 mouse spleens analyzed per genotype. **(G)** Stained sections in F were analyzed with the Leica LAS-AF software. The size (area in μm^2) of 10–15 randomly selected germinal centers from each mouse of the indicated strain was measured. Spleen sections from 4–5 6 mo old mice were analyzed per group. Each symbol denotes one GC. **(H)** Quantitative RT-PCR analysis of mRNA transcripts of the indicated genes in sorted $CD4^+CXCR5^{hi}PD\text{-}1^{hi}$ GC Tfh cells from 6 mo old B6, B6.129-SLAM, B6.RIIBKO and B6.129.RIIBKO mice (n = 3–4 mice per genotype). Error bars show mean ± SD. NS= not significant, * $p \leq 0.05$, ** $p \leq 0.01$, *** $p \leq 0.001$ and **** $p \leq 0.0001$ (One-Way ANOVA).

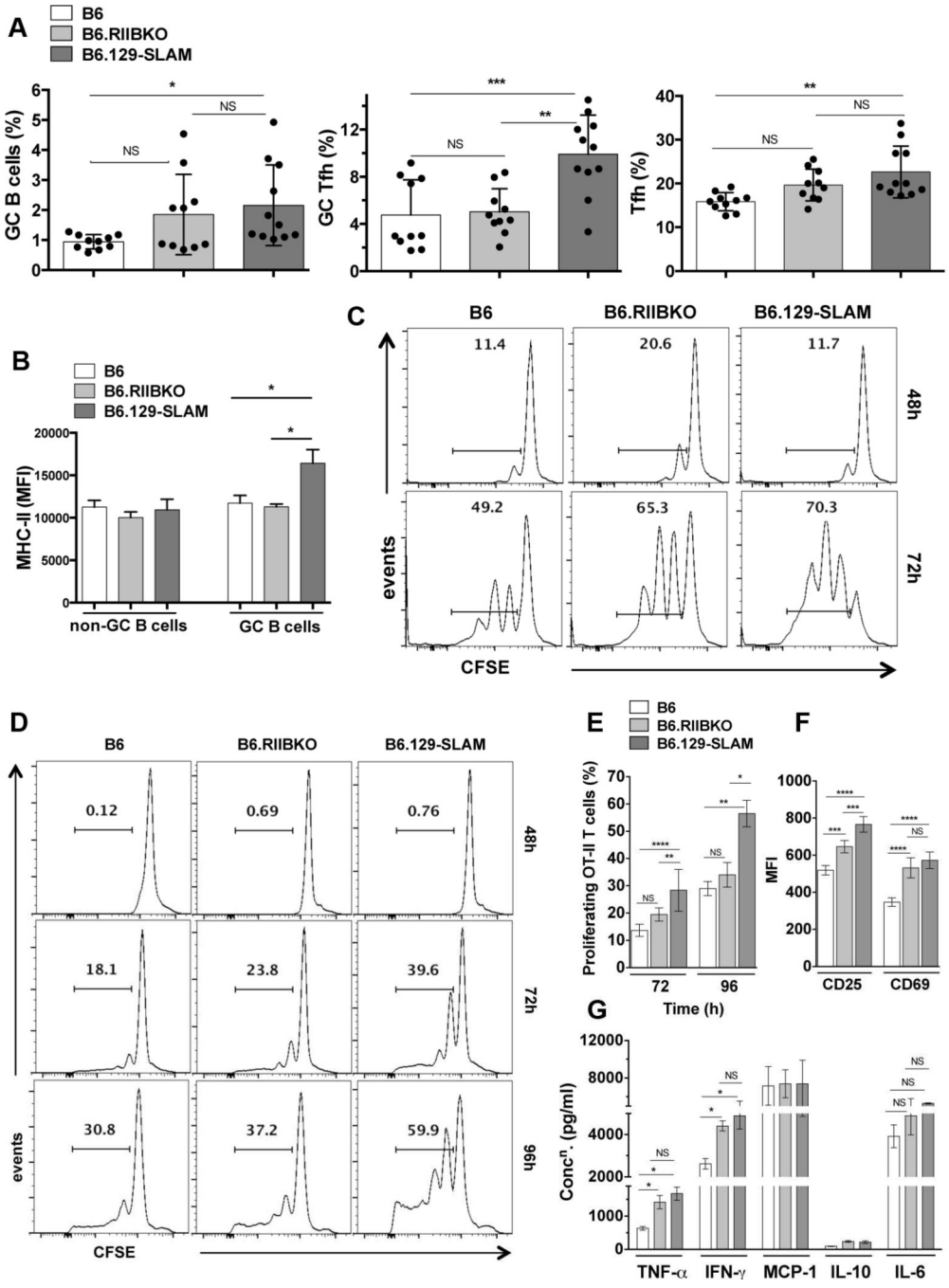

Figure 3. 129-SLAMs promote antigen presentation by B cells and DCs

(A) Scatter plots with bars show the percentages of $B220^{+}PNA^{hi}$ $CD95^{hi}$ GC B cells (left panel), $CD4^{+}CXCR5^{hi}PD\text{-}1^{hi}$ GC Tfh (middle panel) and $CD4^{+}CXCR5^{int}PD\text{-}1^{int}$ Tfh (right panel), in the indicated mouse strains, analyzed from total splenocytes 12 days after immunization with 200μg OVA/ mouse (i.p.). **(B)** Bar graphs show the mean fluorescence intensity of MHC-II expression on non-GC ($B220^{+}PNA^{-}CD95^{-}$) and GC B cells ($B220^{+}PNA^{hi}$ $CD95^{hi}$), measured from mice described in A. These data represent two independent experiments (n = 10). **(C)** B cells from B6, B6.RIIBKO and B6.129-SLAM

mice were differentiated into antigen presenting cells (B cell-APCs) as described in methodology. CFSE labeled purified naïve OT-II T cells were co-cultured with B cell-APCs. Representative histograms show OT-II T cell proliferation by CFSE dilution at 48h and 72h. **(D)** Representative histograms show OT-II T cell proliferation by CFSE dilution at 48h, 72h and 96h after co-culture with BM derived DCs (DC-APCs, described in methodology). **(E)** Percentage of proliferating OT-II T cells as described in D at 72h and 96h of co-culture. **(F)** Bar graphs show the mean fluorescence intensity of CD25 and CD69 surface expression on OT-II T cells co-cultured for 72h with DC-APCs from the indicated mouse strains. **(G)** Culture supernatants from DC-OT-II T cell co-cultures were collected at 72h and analyzed for the indicated cytokines using the flow cytometric cytokine bead array. Data in D-G are from three independent experiments, where DCs were differentiated from BM cells pooled from 3–4 mice per group for each experiment. NS= not significant, * $p \leq 0.05$, ** $p \leq 0.01$ and *** $p \leq 0.001$ and **** $p \leq 0.0001$ (Oneway ANOVA).

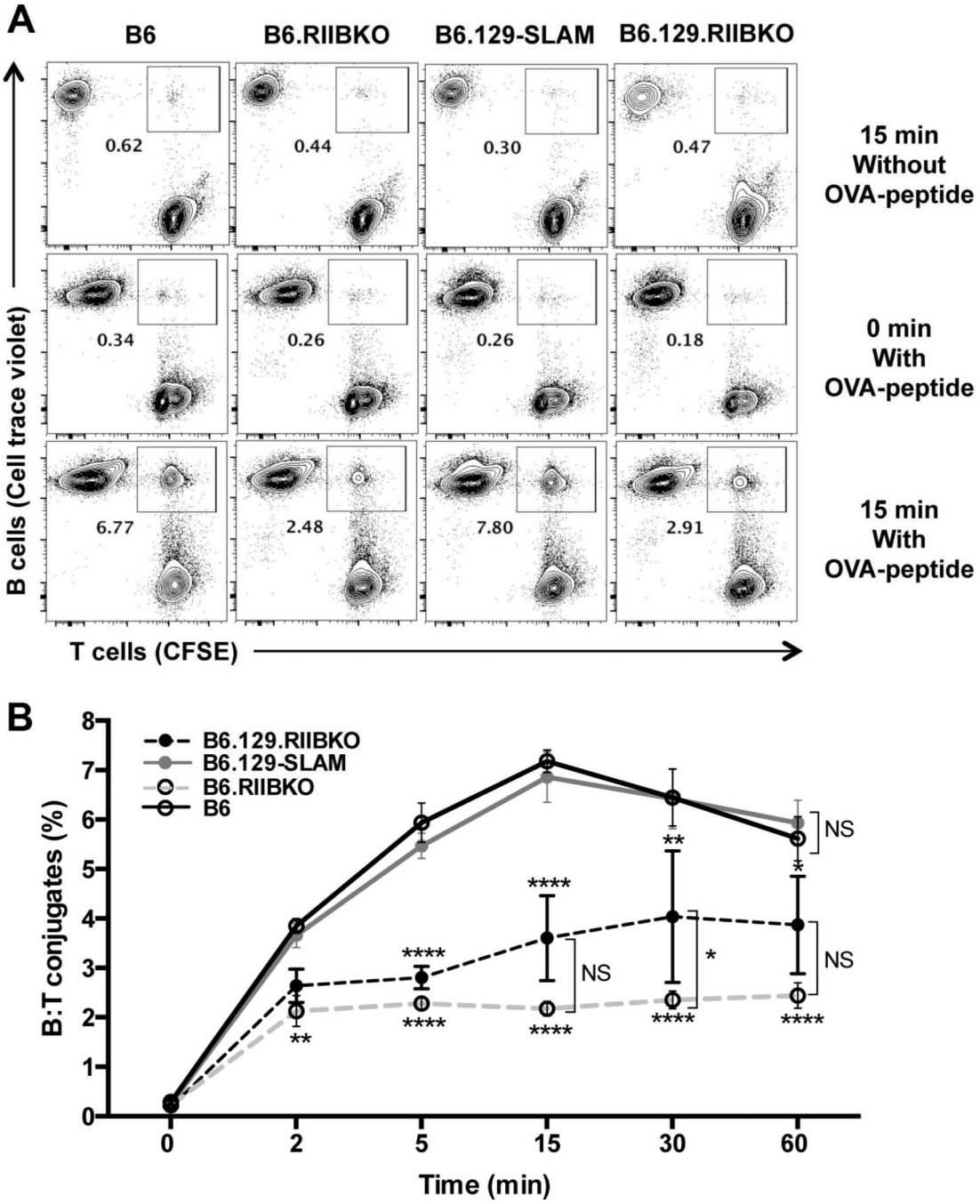

Figure 4. B6.RIIBKO B cells have a lower frequency of B: T interactions

Activated B cells from the indicated mouse strains were intracellularly labeled with cell trace violet and incubated with activated CFSE labeled $CD4^+$ B6.OT-II T cells as described in methodology. **(A)** Representative contour plots show the B: T cell conjugates within rectangular gates at 0 and 15 min time points (middle and lower panels respectively). Upper panels represent negative controls where B cells were not pulsed with OVA-peptide and incubated with OT-II T cells for 15 min. **(B)** Kinetics of the percentage of B: T conjugates formed over the course of 60 min. Data are compiled from 5 independent experiments,

wherein B cells were pooled from 3–4 mice per group for each experiment. Error bars represent mean ± SD. NS= not significant, * $p \leq 0.05$, ** $p \leq 0.01$ and **** $p \leq 0.0001$ (Two-way ANOVA).

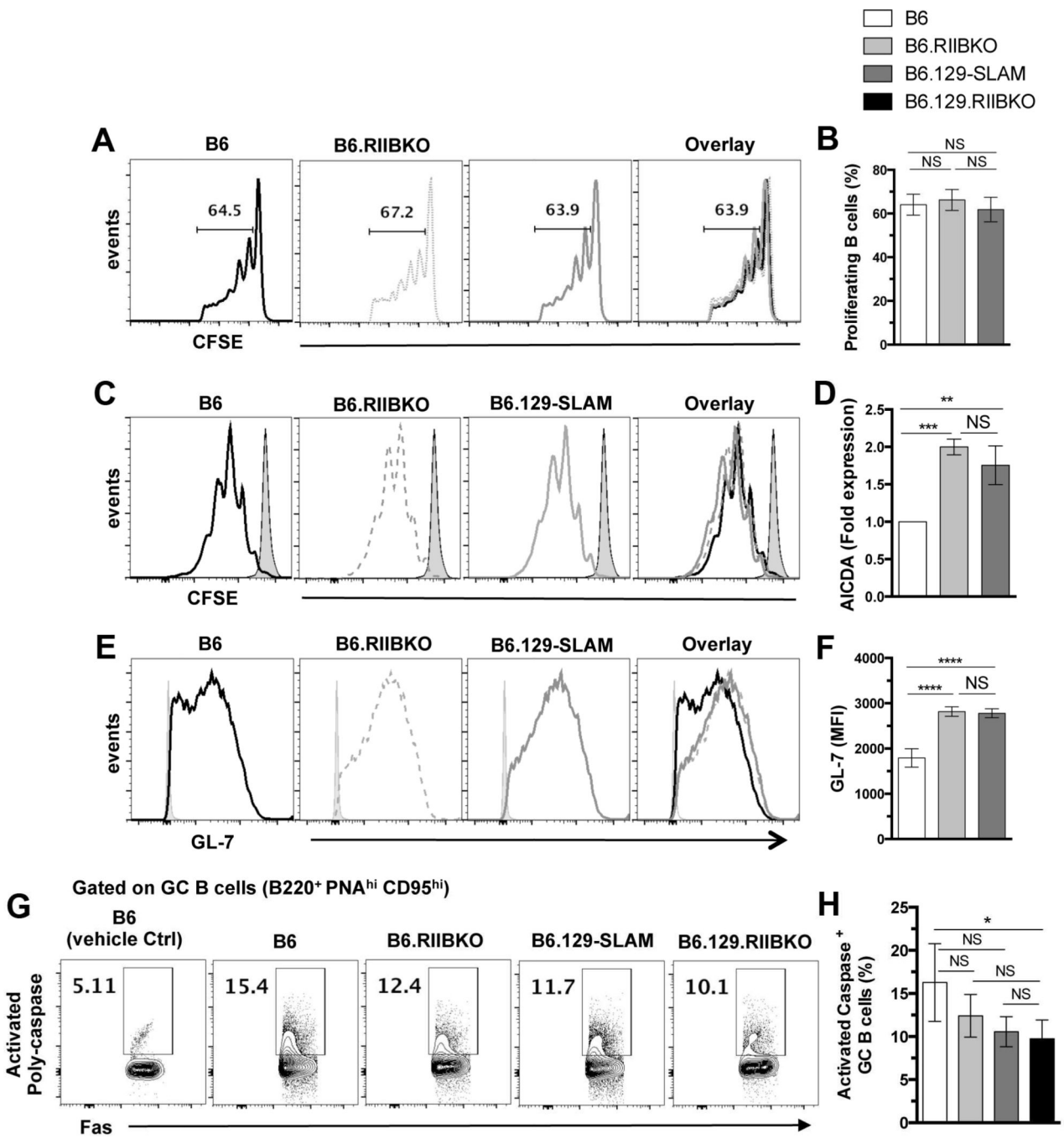

Figure 5. FcγRIIB deficiency and 129-SLAMs do not affect proliferation but promote GC B cell survival and differentiation

(A) Purified CFSE-labeled B cells from the indicated mouse strains were transferred (i.v.) into SRBC pre-immunized μMT mice. Proliferation of transferred B cells was assessed by CFSE dilution three days after transfer. Histograms represent the B cell proliferation profile from two independent experiments with 5 mice in each group. **(B)** Percentage of *in vivo* proliferating B cells as described in A. **(C–F)** Purified CFSE-labeled B cells from B6 (black line), B6.RIIBKO (grey dotted line) and B6.129-SLAM (grey solid line) were cultured for 4

days on 40NBLB cell line as described in methodology. (**C**) B cell proliferation was assessed by CFSE dilution in the indicated strains (grey solid fill- CFSE stained cells at day 0). **(D)** RNA from the co-cultured B cells was analyzed by quantitative real time RT-PCR for *Aicda* transcripts. **(E)** B cells were analyzed by flow cytometry for the surface expression of GC B cell marker GL-7 as shown in histograms. **(F)** Compiled mean fluorescence intensity of GL-7 expression. Experiments in C-F panels were performed twice with B cells pooled from 3–4 mice per group for each experiment. **(G)** Representative contour plots show the gating strategy for $B220^{+}PNA^{hi}$ $CD95^{hi}$ GC B cells stained *ex-vivo* with SR-VAD-FMK, a poly-caspase probe. **(H)** The bar graph shows the percentage of GC B cells positive for activated poly-caspases. At least five mice were analyzed per group. NS= not significant. * $p \leq 0.05$, ** $p \leq 0.01$, ***$p \leq 0.001$ and **** $p \leq 0.0001$ (One-way ANOVA).

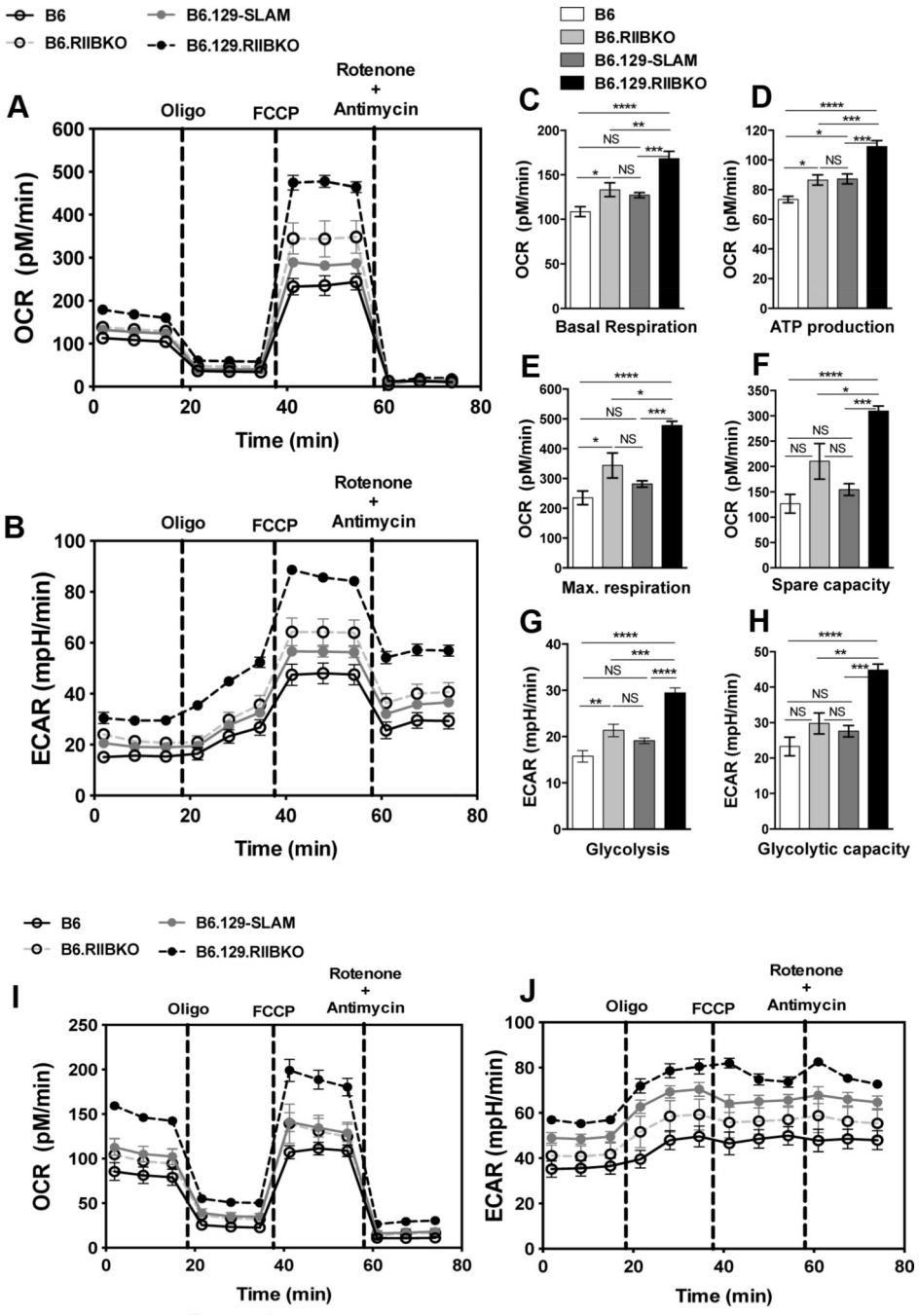

Figure 6. Both FcγRIIB deficiency and 129-SLAMs markedly enhance metabolic activity in B6.129.RIIBKO mice

(A and B) Representative plots show the measurement of OCR and ECAR, respectively, in purified B cells from B6 (solid black line), B6.RIIBKO (dashed grey line), B6.129-SLAM (solid grey line) and B6.129.RIIBKO mice (dashed black line) upon indicated treatments. Histograms show the average basal oxygen consumption **(C)**; ATP production through ATP synthase **(D)**; the maximal electron transport capacity **(E)** and the maximum respiratory spare capacity **(F)** of purified B cells isolated from the indicated mouse strains. **(G and H)**

Histograms depict the average ECAR values for glycolysis and the glycolytic capacity, respectively, of naïve B cells isolated from indicated mouse strains. **(I–J)** Representative plots show the measurement of OCR (**I**) and ECAR (**J**), in purified B cells from B6 (solid black line), B6.RIIBKO (dashed grey line), B6.129-SLAM (solid grey line) and B6.129.RIIBKO mice (dashed black line), activated with anti-IgM and anti-CD40 for 18h and subsequently subjected to the indicated treatments. Data were compiled from two independent experiments with 3–4 mice per group. Each B cell sample was run in at least 5 replicates per experiment. Error bars show mean ± SEM. NS= not significant, * $p \leq 0.05$, ** $p \leq 0.01$, *** $p \leq 0.001$ and **** $p \leq 0.0001$ (One-way ANOVA).

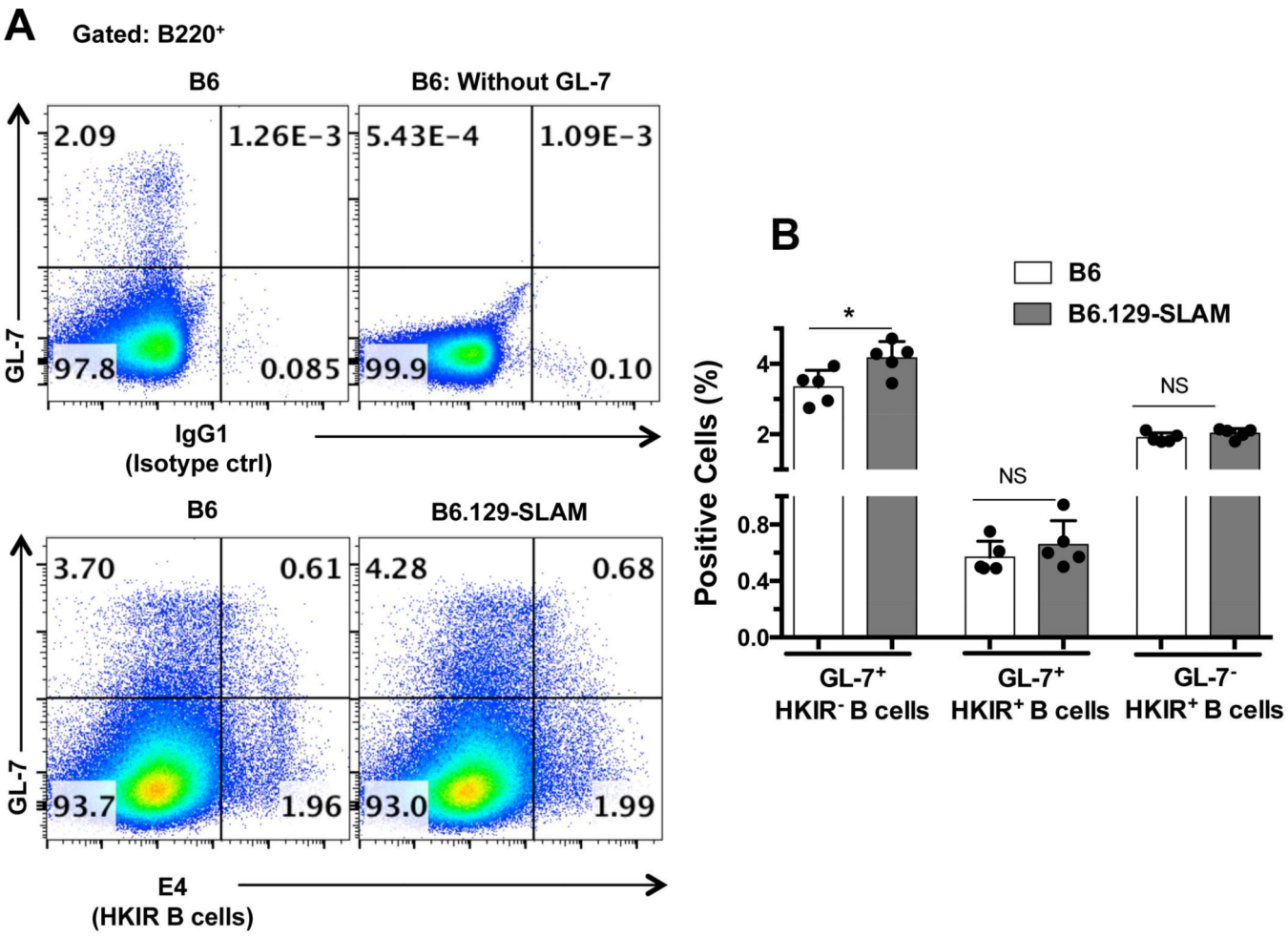

Figure 7. 129-SLAM expression only on T cells and DCs is not sufficient for the recruitment of autoreactive B cells into GCs

Ars-KLH pre-immunized B6 or B6.129-SLAM mice received 2×10^6 HKIR B cells (i.v) (details in methodology). Flow cytometric analysis was performed on splenocytes isolated from these mice where splenocytes were stained with the anti-idiotypic mAb E4 or IgG1 isotype control Ab in combination with GC B cell markers B220 and GL-7. **(A)** Upper panels are representative controls for E4 Ab staining (IgG1 isotype control) and GL-7 Ab staining. Lower pseudo-color plots represent the gating strategy used to define the percentage of HKIR $E4^+$ cells with GC B cell phenotype (top right quadrant), HKIR $E4^+$ cells outside the GCs (lower right quadrant) and non-HKIR $E4^+$ cells within the GCs (top left quadrant) in the indicated mouse strains. **(B)** Histograms show the percentage of cells in each population as defined in A. Each symbol represents an individual mouse and error bars represent mean ± SD. NS= not significant, * $p \leq 0.05$ (Mann-Whitney t-test).

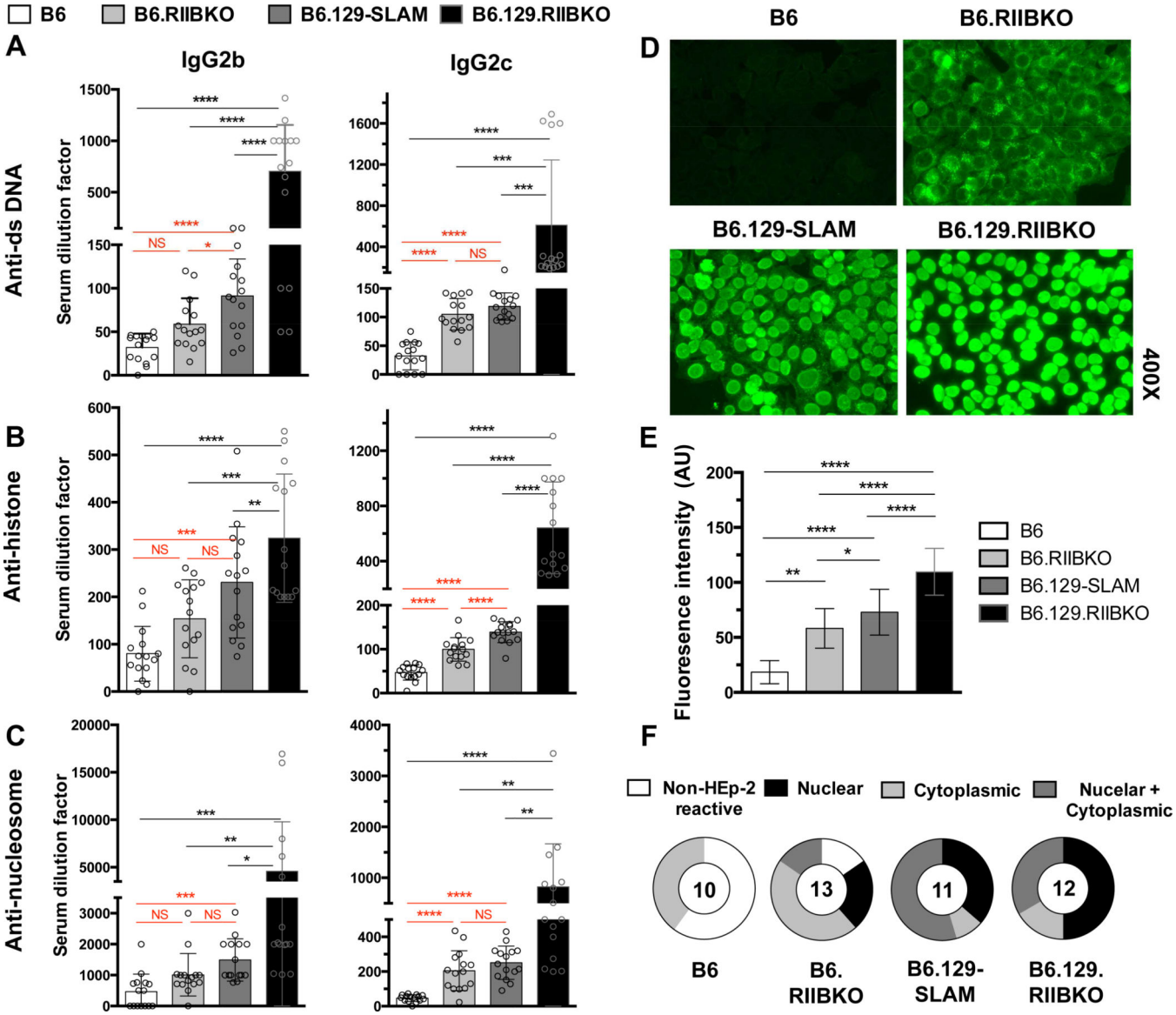

Figure 8. Both FcγRIIB deficiency and 129-SLAMs contribute to the ANA production in B6.129.RIIBKO mice

(A–C) Antibody titers of IgG2b (all left panels) and IgG2c (all right panels) against **(A)** dsDNA; **(B)** histone; **(C)** nucleosome were detected by ELISA, in sera from 6 mo-old female mice. Each symbol represents an individual mouse. **(D)** ANA detection by fluorescence microscopy, using HEp-2 culture slides incubated with sera (1:50 dilution in PBS) from the indicated mouse strains. The images represent the most common staining pattern observed from at least 10 sera samples analyzed per strain. **(E)** Bar graph shows total ANA fluorescence intensity, compiled from all of the HEp-2 staining represented in D. **(F)** Pie charts summarize percentage of mice showing non-reactivity to self (Non-HEp-2 reactive, white); or reactivity to nuclear (black), cytoplasmic (light grey) or both nuclear and cytoplasmic Ags (dark grey). Numbers at the center of the pie chart denote the number of sera samples analyzed per strain. Errors bars in A-C and E show mean ± SD and every

symbol represents an individual mouse. NS= not significant, * $p \leq 0.05$, ** $p \leq 0.01$, *** $p \leq 0.001$ and **** $p \leq 0.0001$ (One-way ANOVA).

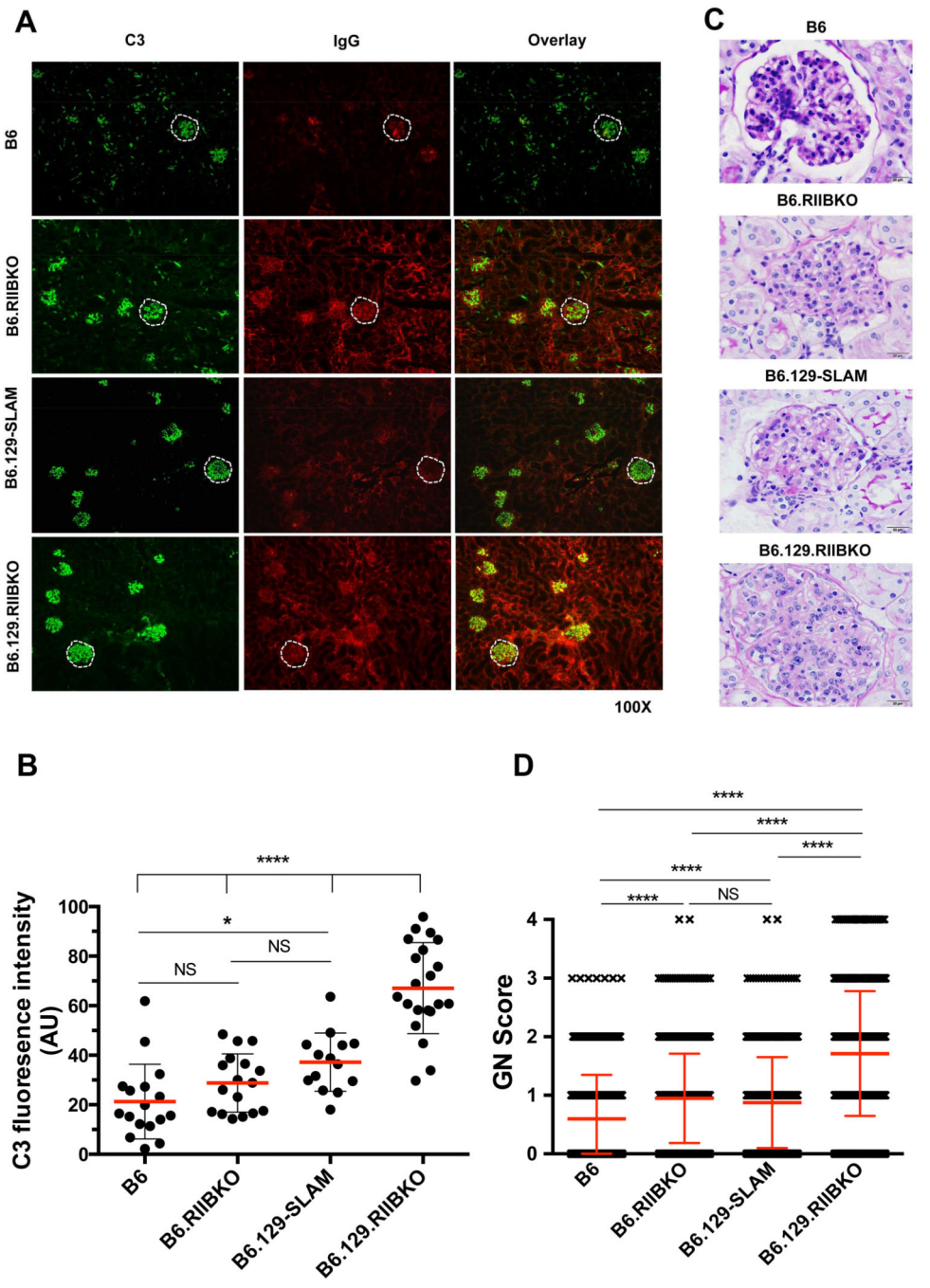

Figure 9. FcγRIIB deficiency and 129-SLAMs promote autoimmunity-associated renal pathology

(A) Glomerular immune complex and C3 deposition were assessed in kidney sections from the indicated mouse strains by immunofluorescence staining for C3 (green, left panels) and IgG (red, middle panels). A representative glomerulus in each section is highlighted within the white dotted line. The images are representative of both the right and left kidney sections from at least five 7 mo-old female mice per strain. **(B)** Stained kidney sections in A were analyzed with the Leica LAS-AF software quantitation tool. The fluorescence intensity of C3 staining in 15–20 randomly selected glomeruli from each indicated mouse strain was

quantitated. Each symbol denotes C3 fluorescence intensity of one glomerulus. **(C)** Representative histology images show glomeruli from kidney sections of the indicated mouse strains stained with periodic acid-Schiff stain (PAS) (scale bars, 20 μm). Six 7–9 mo-old female mice were analyzed per group. **(D)** At least 1000 glomeruli were individually analyzed by a pathologist blinded to the genotypes from PAS stained kidney sections of six 7–9 mo-old female mice per genotype and the mesangioprolferative changes in glomeruli were scored as described in the methodology. Error bars show mean ± SD. NS= not significant. **** $p \leq 0.0001$ (One-way ANOVA).

Table 1

Comparative analysis of total cell numbers of GC B cells, GC Tfh and Tfh.

Cell subset	B6	B6.RIIBKO	B6.129-SLAM	B6.129.RIIBKO
GC B cells ($B220^{+}PNA^{hi}CD95^{hi}$)	0.23 ± 0.43	1.049 ± 0.327	1.181 ± 0.273	2.675 ± 0.614
GC Tfh ($CD4^{+}CXCR5^{hi}PD\text{-}1^{hi}$)	0.395 ± 0.055	0.655 ± 0.19	1.476 ± 0.133	3.144 ± 0.543
Tfh ($CD4^{+}CXCR5^{int}PD\text{-}1^{int}$)	1.19 ± 0.102	2.271 ± 0.565	3.658 ± 0.179	6.660 ± 1.366

Flow-cytometric analysis of total cell numbers (x 10^6 ± SEM) of indicated cell subsets from the indicated mouse strains (n = 5 per group).